CHAPTER 6

Wind-Aided Fire Spread

F. E. FENDELL AND M. F. WOLFF
Space and Technology Division, TRW Space and Electronics Group, Redondo Beach, California

I. INTRODUCTION

Fire spread in wildland encompasses very complicated phenomena, typically entailing turbulent reacting flow and intricate fuel arrangement, with processes

Forest Fires

occurring over a wide range of scales. Consequently, even simple observations and measurements are difficult, and replication is almost impossible. We present here one approach to quantifying such challenging phenomena by undertaking controlled, replicable laboratory-scale experiments which capture at least some of the important phenomena of large-scale fire spread. We then develop a semi-empirical process-based model to simulate wind-aided fire spread and test the model by using the laboratory-scale experimental setup to generate additional data for comparison. The model may subsequently be validated in large-scale wildland fires; when a model which incorporates the key features of laboratory-scale fire spread is applied to a large-scale test, attention must be concentrated on those additional phenomena that did not play a significant role in the smaller scale testing (e.g., see Chapter 8 in this book).

In general, a small number of extreme fire events is responsible for most of the total area burned [e.g., 10% of the fires in southern California account for over 90% of the area burned (Minnich, 1998)]. Thus, we focus on extreme conditions of very dry fuels and high winds which may result in exceptionally high-intensity, rapidly spreading fires *involving surface fuels*. The objective is to predict the spread of such wind-aided fires (i.e., given the current location of the firefront and given requisite information about the adjacent unburned region prior to front arrival, where will the firefront be at future times?). Traditional approaches to this problem have constrained the firefront perimeter to an elliptical shape (see Finney, 1998) or used percolation theory (Christensen *et al.*, 1993) to speculate about probabilities of future locations of the firefront. However, such approaches often delve little into physical mechanisms and may not readily permit the incorporation of observational data. Given the difference in our current state of knowledge concerning low-intensity and high-intensity fire, we do not think that it is a wise investment of effort to try to develop a tractable fire spread model that would be applicable in all situations. Therefore, our model focuses on exceptional conditions conducive to the initiation and persistence of rapid wildland fire spread (i.e., fire spread across dry, moderately sparse fuel under fairly sustained substantial wind of fairly constant direction). Such conditions are exemplified by, for example, Santa Ana-wind-driven fires in southern California chaparral (Pyne, 1982; Reid, 1994; Goldstein, 1995) and related fires arising in other Mediterranean-climate locales (Table 1; Figure 1).

For idealized scenarios, the travel of the firefront in time is straightforward (Richards, 1993). For a uniform fuel distribution on level ground in the absence of wind, an initially circular front advances with radial symmetry and remains circular (Figures 2a and 2b). For a uniform fuel distribution on level ground in the presence of a near-ground (say, at 10-m height) wind that is steady in magnitude and constant in direction, a firefront growing from a localized ignition often becomes oval in shape (Figure 2c). The head of the fire (where the propagation is with the wind) spreads relatively rapidly, the back or rear of the fire (where the propagation is against the wind) spreads relatively

TABLE 1 Sites of Wind-Aided Spread in Mediterranean Fire Regimes

Site	Typical vegetation	Typical wind	Notes
Southern Hemisphere			
Chile (central)	matorral (underbrush)	upslope	no strong coastward wind
South Africa (near Cape of Good Hope)	fynbos (small bush)	berg (foehn wind blows coastward)	4–24-year cycle of regeneration
Australia (NSW, Victoria, South Australia)	mallee (shrub-like eucalypt)	off interior desert, often followed by cold southerly burster	degraded soil, modest hills, occasional summer rain; SW Australian fires not strongly wind-aided
California			
Northern	chaparral (scrub oak; chamise, manzanita)	Mono	20–40-year cycle of regeneration, hilly terrain
Southern		Santa Ana	
Mediterranean Basin			
Greece, Spain, France	maquis (high shrub) garrigue (low shrub)	bora (dry cold winter wind off Julian Alps toward Adriatic); sirocco (dry hot South spring wind—Italy, Spain); mistral, tramontane (dry cold NW wind off Alps toward Gulf of Genoa—France, Spain)	hilly terrain
Greece, Spain	phrygana (Greece) tomillares (Spain) (dwarf shrubs)		
Spain	matorral (underbrush)		
Italy	macchia (shrub zone)		

slowly, and the flanks (where the propagation is across the wind) progress only moderately differently from the rate for the no-wind conditions. Clearly it is the component of the wind which is locally perpendicular to the fire perimeter that establishes whether advection carries or inhibits the travel of hot product gases from just-burned fuel over the next-to-burn fuel to help preheat it. The long axis of an oval fire perimeter typically continues to increase more rapidly than the short axis. An oval perimeter frequently is narrower at the head than at the rear (where the width is the dimension perpendicular to the wind direction), and the width is often maximal near that windward site (along the bisector of the burned area) that marks the point of origin. "In uniform fuel under constant environmental conditions, the local rates of spread can be expected to be

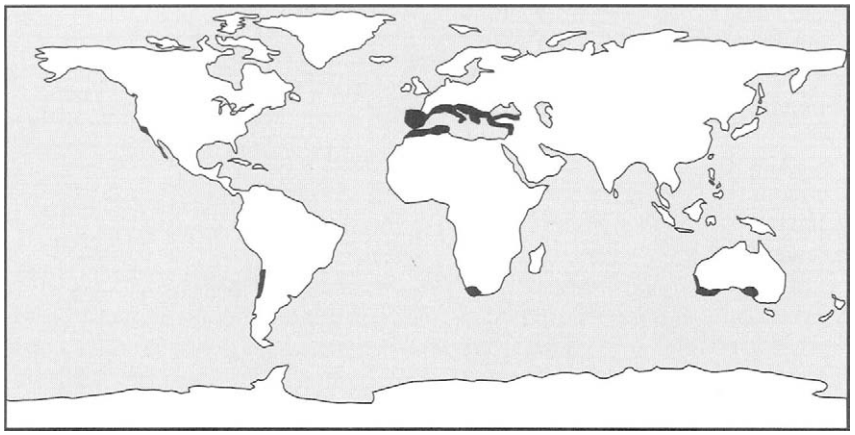

FIGURE 1 Mediterranean climate locales, in which near-coastal scrublands typically have low-fertility soils, and in which fire spread through surface vegetation is seasonally encountered, include southern California, central Chile, much of the Mediterranean basin, the Cape region of South Africa, and Australia (especially South Australia and Victoria).

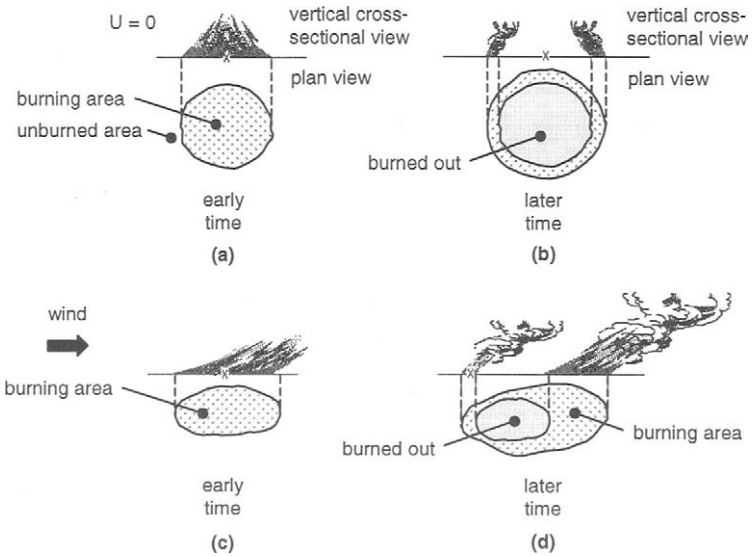

FIGURE 2 (a) At an ignition site in a uniform expanse of unburned fuel on level terrain, under calm, a firefront (which propagates slowly outward, against convectively induced advection) evolves to demarcate (b) an interior region with burned-out thin fuel, from an exterior region of unburned fuel. (c) For the corresponding event in the presence of a near-ground ambient wind sustained in magnitude and direction, the firefront evolves to an oval configuration. (d) The rate of propagation is appreciably enhanced along the portion of the perimeter where the wind aids spread and inhibited where the wind opposes spread. The enhanced spread occurs due to hot combustion-product gases preheating unburned downwind fuel.

constant for head, flanks, and back of fire. Thus the area burned over per unit time can be expected to grow linearly with time, the perimeter expected to grow at a steady rate, and the actively burning area inside the perimeter to grow in proportion to the perimeter" (Albini, 1992, p. 44).

The oval shape of the firefront perimeter arising in simplistic scenarios has been taken by many researchers to have the special configuration of an ellipse (see Finney, 1998, and references cited therein). There seems no fundamental reason for the elliptical shape to hold; in fact, the ellipse is but approximately representative of the firefront perimeter, even for burns under uniform conditions (Pyne *et al.*, 1996, pp. 58–59). Nevertheless, it is virtually unavoidable that reference to ellipses permeate the ensuing discussion of the firefront-perimeter literature. Because of the emphasis sometimes placed on elliptical configuration for the firefront in wildland vegetation, we note that there are parameter ranges for which the firefront is *not* even roughly elliptical, despite high regularity of the fuel distribution, virtual flatness of the terrain, and constancy of the wind magnitude and direction. In the hummock grasslands of arid Western Australia, the patchy fuel distribution admits fire spread only for winds above a finite significant threshold of 3–5 m/s or so (at 2 m height). Under a strong wind, backing fire spread is minimal, flanking fire spread is modest, and head fire spread from a localized ignition results in a downwind-widening-wedge shape for the burned clumps of vegetation (Burrows *et al.*, 1991; Gill *et al.*, 1995; Cheney and Sullivan, 1997). Because the burning of these spinifex plains, for which 30–50% of the ground may be covered by spinifex-type grass (with the remainder being bare arid soil), raises significant issues, we return to spinifex later.

Of course, in realistic scenarios, neither the wind, fuel loading, nor topography remains constant, and no useful general statement about how the configuration of the fire perimeter evolves seems likely to hold. The nonuniformities result in a typical, convoluted fire perimeter (in a plan view, Figure 3) having concavities (indentations called "pockets") and convexities (protrusions called "fingers") (Pyne, 1984); the possibilities are myriad. For example, buoyancy induces a wind that aids upslope spread and inhibits downslope spread; yet, if the ambient wind were blowing across the slope, then what might be considered a flank on the basis of slope might become a head on the basis of the forced convection. Such reorientation is also to be expected if the wind alters direction, as apparently is commonly encountered in southeastern Australia bush fires when sirocco-type winds, drawn off the hot desert interior prior to cold-front passage, are succeeded by cooler moister southwesterly winds (southern burster) off the ocean after cold-front passage (Pyne, 1991). Corresponding reorientation is less common in southern California because weather fronts pass to the north, especially in dry years. However, at the end of Santa Ana-wind-driven fire spreads in southern California, during which compressionally heated dry winds descending off the Colorado plateau accelerate through narrow passes in the southern Sierra Mountains to cause rapid propagation from the interior toward

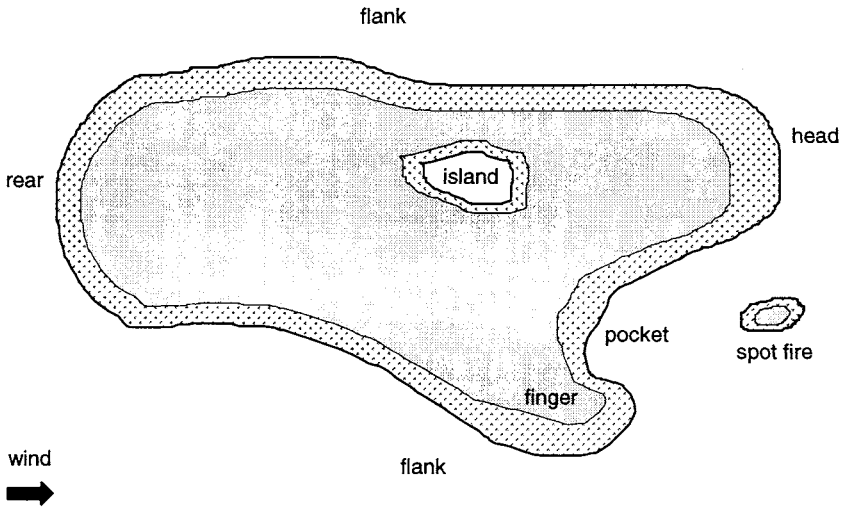

FIGURE 3 Some commonly used terminology to describe phenomena associated with wind-assisted fire spread through wildland fuel and portions of the firefront perimeter.

the coastline, the eventual return of gentler onshore marine winds may lead to a daytime reversal of the direction of spread. If so, patches of fuel (islands or "refugia") left unburned may then be consumed (Pyne, 1995). Since (as with other relevant parameters) the slope of the terrain is perennial but exceptionally rapid fire spread is dominantly strong-wind-associated, we infer that wind incrementation of spread rate can appreciably exceed slope incrementation. Accordingly, the emphasis here is on fire spread under windy conditions.

II. LABORATORY-SCALE SETUP

We regard the conducting of well-instrumented experiments to be an essential part of wildland fire modeling. In accord with Emmons (1971), we place emphasis on the control of experimental conditions to yield reproducible results. The requirements for studying fire spread in a wildland situation are appreciable: sensor distribution, maintenance, and readout; the area of surveillance and the need for periodic updating of fuel properties and quarter-hourly (if not subminute) updating of weather data; the requisite information collection, storage, processing (including interpolation and extrapolation of the input data from specific monitored sites to encompass the entire field of interest), display and distribution. Furthermore, the obvious dangers of working in the types of uncontrolled extreme wildfires of interest preclude the intentional execution

of such events. Also, as mentioned previously, without adequate controls of the various variables such as fuel loading, moisture content, and wind speeds, it is difficult to test the roles of these factors. Finally, wildland fire situations are difficult to replicate. For these reasons, we have taken the approach of conducting laboratory-scale experiments to develop and test a fire spread model. We use fuel beds of regularly arranged discrete fuel elements that are well-defined, with properties that can be systematically varied.

A. Test Facility

Although a test facility with a large cross-sectional area is preferable, the larger the cross section, the bigger is the blower needed to generate the wind that permits examination of flow-assisted fire spread. The cost to build and operate the facility increases with size; this can defeat the objective of extensive use of the facility for data collection for the multiparametric phenomena of interest. A list of international laboratory facilities for testing wind-aided fire spread across discrete-fuel beds is given by Pitts (1991).

We prefer a facility that blows the airstream from upwind, through the test section and over the test bed of fuel. Sucking air from the downwind side of the test section is a laboratory artifice that inhibits the entrainment of air from downwind into the hot, buoyant firefront gases (Cheney and Sullivan, 1997, pp. 80–81).

We also prefer a facility with a movable ceiling that can translate in the direction of the wind (Figure 4). Buoyant firefront gases may rise with a minimum

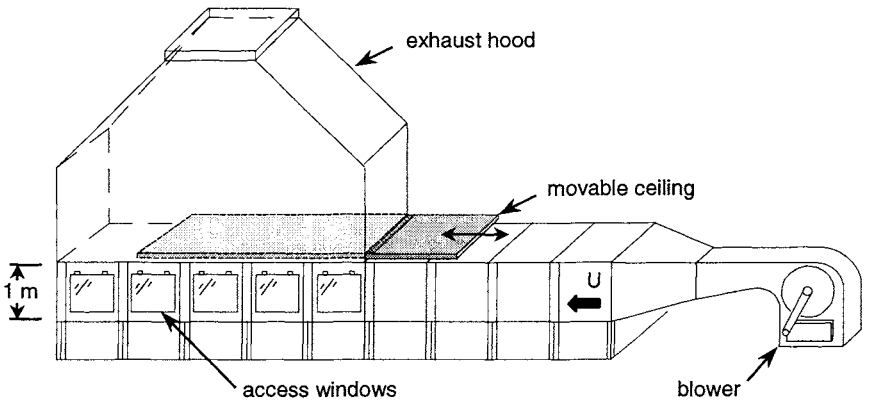

FIGURE 4 Sketch of a wind-tunnel facility with a blower that pushes ambient air through a flow-conditioning section, to produce an approximately uniform stream of low-turbulence air. The approximately 1-m-wide, 5-m-long test section has a movable ceiling that can translate in the direction of the wind.

of obstruction if the downwind edge of the ceiling is dynamically positioned just upwind of the propagating firefront. A movable ceiling maintains a constant cross-sectional area for the portion of the test section that is upwind of the propagating firefront so that the speed of the wind arriving at the firefront remains invariant with firefront advance. Mounting of a video camera at the downwind end of the ceiling furnishes feedback for positioning the ceiling during a test and also provides an excellent overview. The height for a fixed ceiling to be nonintrusive (so hot product gas is not artificially forced over the downwind, still-unburned portion of the fuel bed) is uncertain. Since the height of the visible flames during testing in our facility (to be described later) is typically a meter or two, a factor-of-ten "clearance" would require a blower capable of supplying winds in excess of, say, 5 m/s for a test section 10–20 m in height! Alternatively, if the wind from the blower is allowed to expand into a test section with a cross-sectional area much larger than that of the flow-preparation duct so that the test section is effectively without a ceiling, then the wind speed decreases along the length of the test bed. Only with a movable ceiling is a quasi steady rate of propagation in a uniform wind speed achievable, if a quasi steady rate exists for the given conditions. Data from our facility show that the rate of fire spread is significantly increased when the ceiling height is held constant at 1 m relative to results obtained for the same conditions with the movable ceiling; also, the rate of fire spread is slowed for results obtained for testing without deployment of the ceiling, so the blower-generated wind expands into a very large test section (Wolff *et al.*, 1991, Figure 9). To our knowledge, our facility is the only one with a movable ceiling, and Table 2 indicates that fire spread rates obtained in it are less than corresponding rates measured in other facilities with fixed ceilings. We omit citation of qualitative sketches from the compilation included in Table 2.

B. Instrumentation

We concentrate exclusively on seeking the fire-propagation rate as a function of the prefire fuel-bed observables, taken as uniform in space, and of the wind, taken as constant in time. The observables include (1) the initial fuel loading, (2) the fuel height, (3) the thickness of fuel elements, (4) the fuel moisture, (5) the fuel-bed width, and (6) the wind speed.

To measure the rate of fire spread, we use type-k, chromel–alumel thermocouples inserted at regular intervals (along the centerline of the fuel bed, in the direction of the wind) from underneath so that they protrude up through the bed. The response time of the commercial thermocouples (OMEGA, Stamford, CT) is about 1 s—adequate since the typical propagation rate is observed to be below 10 cm/s.

TABLE 2 Fire Spread Rate v_f Dependence on Wind Speed U ($v_f \sim U^n$)

Researcher	n exponent, U^n	Fuel type	Scale
Thomas (1971)	0.42–0.65[a]	heather and gorse	field
Wolff *et al.* (1991)	0.49[b]	white pine toothpicks	lab
Fons (1946)	0.67[a]	ponderosa pine twigs	lab
Steward (1974)	0.84[a]	poplar wood shavings	lab
Steward and Tennankore (1979)	0.9–1.9[a]	birch dowels	lab
Catchpole *et al.* (1998)	1[b]	regular and coarse excelsior, ponderosa pine needles/sticks	lab
Gould (1991)	1[b]	kerosene/eriachne grass	field
Marsden-Smedley and Catchpole (1995)	1.31[b]	buttongrass	field
Steward (1974)	1.38[a]	poplar match splints	lab
Nelson and Adkins (1988)	1.51[b]	slash-pine needles	lab
Rothermel (1972)	1.9[c]	$\sigma = 97.7\ \text{cm}^{-1}$	model (semi-empirical)
Burrows (1999a)	2.22[b]	jarrah litter	lab
Burrows (1999b)	2.67[b]	jarrah litter	field

[a]Data interpretation performed by Wolff *et al.* (1991).
[b]Data interpretation performed by the researchers themselves.
[c]Data interpretation performed by Gould (1991).
Note: The symbol σ denotes surface-area-to-volume ratio.

The time histories of the centerline thermocouples are used to ascertain when and where a quasi steady rate of fire spread is achieved, and what that rate is. Quasi steady propagation is achieved if the time history of a centerline thermocouple is effectively identical to those of its neighbors, with temporal offsets based on spatial separation. A typical thermocouple time history involves

1. A slow rise in temperature (interpreted as preheating);
2. A subsequent, more rapid rise (interpreted as onset of flaming); and finally
3. A gradual fall (interpreted as forced-convective cooling of the thermocouple owing to the blowing).

Thermocouples are relatively inexpensive, are easily connected to a data-acquisition system, and furnish data readily processed via automated (computer) analysis, in contrast with video or infrared-camera recordings.

Thermogravimetric analysis (TGA) of white-pine toothpicks (the basic fuel type used in our laboratory testing) indicates that 70% of the mass evolves as gas (via pyrolysis) during gradual heating from 575 to 675 K. The speed and

turbulence level of the oncoming wind are determined by hot-wire anemometry. The moisture content within the fuel is determined by weighing the fuel before and after drying.

III. FIRE SPREAD MODEL

Using the previously described test facilities provides measurement of spread rate as a function of the various test parameters; the results also guide our thermo-gas-dynamic modeling of wind-aided fire spread.

A. Properties of the Model

Directly applying the conservation of mass, momentum, and energy to the fuel bed and atmosphere for tracking the progression of the firefront is very difficult. The highly disparate spatial scales, intricate geometry, and unsteady motion remain formidable obstacles. Typically, all cumulatively significant phenomena occurring on scales smaller than the computational grid scale are parameterized (phenomenologically formulated) in terms of grid-scale variables. In general, it is unknown whether a valid representation of such kind is even possible, and, even if possible, such representation is usually not known. Validation of adopted conjectures requires detailed comparison of predictions with observations in a multitude of cases, and this demanding exercise is rarely carried out.

Instead, an approximate *semiempirical* model of firefront-propagation phenomenology is sought (Beer, 1990, 1991). For such a model to be useful in practice, the inputs should require no more detail concerning the local topography, meteorology, and combustible matter than would normally be available. Our objective is to predict the position of the firefront (idealized as a mathematically thin interface) at a later time from knowledge (1) of its position at an earlier time and (2) of a *minimal* amount of (plausibly available) information about essential properties of the environment in the vicinity of the firefront. In treating the firefront as an interface, we are tentatively regarding estimation of firefront thickness and time for thin-fuel-element burnout as lower priority issues.

We concentrate here on a single firefront from a single ignition; nevertheless, the firefront, owing to the presence of firebreaks, spotting, or other circumstances, might become multiply-connected. Thus, burned-over areas should be tallied, lest repeated burning of the same fuel owing to shifting wind (or merger of two initially distinct firefronts) be erroneously permitted. Furthermore, the firefront need not be a closed curve at any time, but we deal with the closed-curve case here.

For typical southern-California-hillside scenarios, the (immobile) combustible matter consists predominantly of shrubs, such as chamise and manzanita, and small trees. There is no noteworthy organic matter in the soil and no noteworthy overstory of crowns. Thus, we focus exclusively on predicting firefront propagation through surface fuels and give a lower priority to predicting flame height. Because the time for flame to progress from one discrete fuel element to another is much less than the temporal resolution of practical interest, we may treat the distribution as an effectively continuous, equivalent mass of combustible matter per unit planform area. Accordingly, we infer the progress of the firefront to occur smoothly, not in discontinuous jumps.

Undertaking a simple approach first, we take the dependence of the firefront-propagation speed to be on the values of local parameters, not on the spatial or temporal gradients of the parameters. Nevertheless, the value of any parameter is permitted to change in space and/or time. The procedure entails a quasi steady approximation in that the flame speed holding for a given set of parameter values is instantaneously equilibrated to that set of values, whatever the antecedent set of values. That is, if we regard the instantaneous firefront as a perimeter of ignition sites, the rate of fire spread is taken instantaneously to reach the equilibrium rate of spread (into *unburned* fuel) for the local values of the parameters related to propagation.

We do not incorporate spotting, the discontinuous mode of spread associated with the lofting of firebrands. If the fuel distribution varies but moderately ahead of the current firefront position, then neglect of short-range spotting typically results in a modestly inaccurate rate of spread, since the firefront probably soon arrives at the brand-ignited site by the continuous mode of spread. Longer range spotting may permit the fire to traverse effectively fuel-free expanses that would constitute firebreaks for the continuous mode of spread. We do not address the interaction of the fire with the environment, so the nominal environmental conditions are the conditions adopted for use in the model. For example, any alteration of the wind by transit of already-burned-over expanses of fuel is taken to be a higher order effect in describing the wind arriving at the currently burning fuel. This simplification is anticipated to require modification in some circumstances. However, ignoring fire modification of the wind typically may furnish an overprediction of spread rate, so the consequences are known. We also do not explicitly incorporate the consequences of fire fighting on the firefront-propagation model (e.g., owing to air-tanker or helicopter drops of fire retardant or water on the fuel bed), except as those consequences may be formulated in terms of parameters (such as fuel-moisture or soil-moisture content), plausibly incorporated in the model for intervention-free spread. Of course, tracking the fate of an attempted backfire may be regarded as little different from tracking the firefront progress evolving from any other discrete (independent) firestart.

B. A General Formulation

The firefront (interface) that encloses the area with burned thin combustible matter is denoted by the "simple" smooth two-dimensional, plane-projection curve $\Gamma(s, t)$, where s denotes distance along the curve at time t (Figure 5). We choose the parametric representation such that the burned area lies to the left during a transit of the perimeter in the direction of increasing s. The direction of fire spread through the fuel bed (the movement of the interface), in the immediate vicinity of any point $x_i(s, t)$ on the interface, is perpendicular to the interface. The interface-translation speed F at each point on the interface is taken to depend on the values assigned to the state variables $u^{(j)}$ at that point on the interface at the time of interest. The number of state variables is the minimal number of properties of the fuel bed, the meteorological environment, and the topography necessary for a description (of the interface movement) that is of sufficient accuracy to meet our requirements. Thus, for $t > 0$, with subscript $i = 1$ or 2,

$$\frac{\partial x_i(s, t)}{\partial t} = F\{u^{(j)}[x_i(s, t)], v_i(s, t)\}, \qquad x_i(s, 0) \text{ given} \tag{1}$$

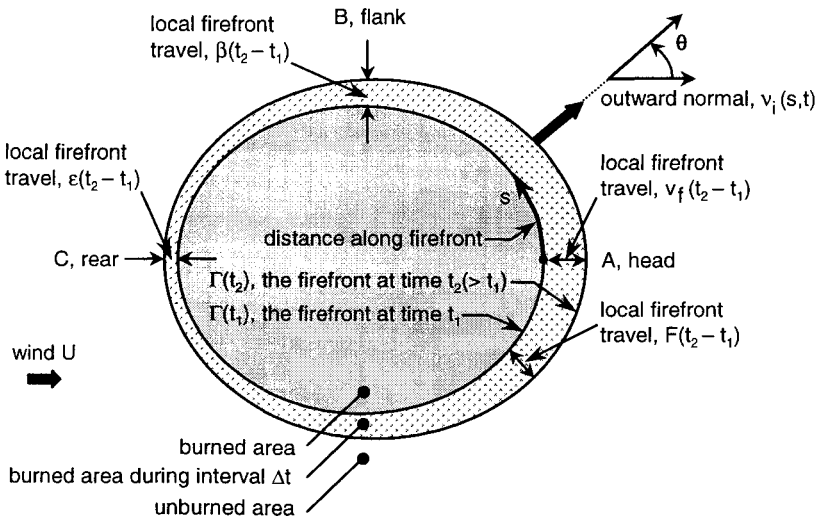

FIGURE 5 A schematic of the increase in burned area (shaded region) due to the firefront travel (stippled region) during the time interval $(t_2 - t_1)$ under a wind of magnitude U in the direction $\theta = 0$. The distance s along the firefront at time t_1 is measured from $\theta = 0$; a corresponding distance may be computed for the firefront at time t_2. The rate of spread F depends (*inter alia*) on the local unburned-thin-fuel loading and the component of wind normal to the front, so F varies with θ. The general rate F takes on the particular values v_f, β, and ε at the head, flank, and rear of the fire, respectively.

where $v_i(s, t)$ denotes the outward normal. We let $x_1(s, t)$ denote the x position at time t of the point s along the perimeter, where x is a Cartesian coordinate along the direction of the time-averaged wind at reference height above the ground; $x_2(s, t)$ denotes the corresponding y position, where the coordinate y is perpendicular to x, in accord with the right-hand convention. We regard the dependence of the functional F on $u^{(j)}$ to be known *empirically*. Only the component of the wind locally normal to the firefront is taken to aid the advance of the local fire perimeter. In terms of the functions of computer software developed by the Fire Sciences Laboratory (Missoula, MT) of the Forest Service, U.S. Department of Agriculture, for a two-dimensional simulation of fire growth through surface fuels: (1) integration of Eq. (1) corresponds to the tasks undertaken by the code FARSITE (Pyne *et al.*, 1996; Finney, 1998); and (2) the *key* functional F is furnished by the code BEHAVE (Rothermel, 1972; Andrews, 1991), which serves as a subroutine for FARSITE. Below we shall address issues concerning mathematical accuracy and real-time implementation for FARSITE, physical-formulation issues for BEHAVE, and limitations of a quasi steady, semi-empirical approach. An Australian analogue of FARSITE is *SiroFire* (Coleman and Sullivan, 1996). Were there sufficient record of the firefront position $x_i(s, t)$ during large fires, we might address the inverse approach of trying to infer the functional F from knowledge of $x_i(s, t)$, but such an undertaking is not currently practical.

This "parametric" model of firefront travel is probably not capable of accurately resolving any fine-scale detail. Thus, in the current context, we ascribe no credibility to details of behavior predicted by the model if the curvature of the boundary is significant, as would be locally the case if the length of the boundary between two points on it were comparable to the local radius of curvature. Thus, prediction of large-curvature behavior is suspect as a mathematical artifact of an approximate incorporation of the physics of the situation in the formulation. How to resolve such artifacts is perhaps best ascertained as one gains experience with the use of the model. To reiterate, the incidence of singularities in curvature [usually a consequence of negative curvature ("pockets" in Figure 3) arising on the fire perimeter] may be the "most fascinating propagation characteristics" (Sethian, 1996, p. 28) mathematically. However, their occurrence may reflect simply an incomplete incorporation of the physical laws.

C. Approaches to Solution of the Formulation

In practice, of course, a finite-difference approximation to the differential equation [Eq. (1)] is solved. A number of marker points distributed around the interface are advanced by stepping forward in time, with a smaller distance be-

tween marker points Δs and a smaller time step Δt (within limits) seemingly likely to incur smaller error because such choices permit a better approximation to the derivative. However, in this approximate formulation, a coarser resolution could conceivably furnish a prediction closer to observation. Simplistic procedures for treating the evolution equation include a first-order Euler time-stepping procedure, or a second-order, predictor-corrector procedure; the order of the numerical method also factors into the numerical error. Roberts (1989) emphasizes a distinction between (1) the advancing of the distributed marker points adopted to approximate the firefront curve at time t and (2) the advancing of line segments adopted to approximate the curve. The distinction seems somewhat blurred in that a line segment must be associated with each marker point in order to define the local normal to the curve, a necessary step to defining the local direction for advancement.

The commonly utilized computational procedure is described as "adopting Huygens' principle" (see, e.g., Anderson *et al.*, 1982; Knight and Coleman, 1993; Richards, 1993, and the references cited therein). The procedure usually amounts to applying an elliptic stencil to describe how the fire grows at marker points and drawing a smooth curve through the most advanced points on the ellipses to obtain the updated location of the interface. The procedure seems arbitrary and not particularly convenient for convoluted perimeters and, in general, possibly highly inaccurate for the intricate nonhomogeneous situations encountered in practice. Huygens' principle is usually encountered in the context of ascertaining the evolution of an acoustic or electromagnetic wavefront. The corresponding conjecture to permit tracking the propagation of a firefront across a fuel bed is taking each point on the perimeter of a large fire to be an ignition site for a new fire, which grows with the shape and orientation of the original perimeter, the result being a larger fire of the same shape (Albini, 1984). In practice, with few exceptions, the result is a larger fire of the same shape (Albini, 1984). In practise, with few exceptions, the adopted firefront shape evolving from an ignition site is always taken to be an ellipse, with the ignition site taken as coincident with rear focus of the ellipse. The commitment to an elliptic firefront evolving from an ignition site on the firefront perimeter implies that some already-burned fuel is treated as if it may reburn—and then may burn once more, because the ellipses from neighboring ignition sites typically overlap. An ignition at the perimeter of a burned-over area is not equivalent to an ignition within an unburned area; the experience that an ignition site evolves to an oval firefront under a wind is derived from observation of spread through an entirely unburned expanse of fuel. An upshot is that, under the just-described Huygens' principle methodology for fire growth, the firefront is not always propagated normal to itself into unburned fuel without *ad hoc* adjustment. Finney (1998, pp. 28, 32) acknowledges that subjective spread-rate adjustment factors are introduced to bring predictions of the Huygens' principle-

based FARSITE model into agreement with observations of fire growth. Adjustment is necessary because spread-rate predictions exceed the observed fire growth for all fuel models treated. It is currently unresolved and perhaps unresolvable whether the discrepancy between prediction and observation is owing to (1) shortcomings in the BEHAVE model of the spread rate for a given set of state variables (see discussion that follows), (2) adoption of the elliptical-stencil methodology to treat the firefront-evolution equation, (3) the spatial/temporal resolution of the data put into the calculation, or (4) the step size used in space and time to advance the solution—or a combination thereof. Finney (1998) suggests that finer resolution in space and time in the modeling will result in closer agreement between prediction and observation. In contrast, Cheney and Sullivan (1997) suggest that, for a heading fire, wind measured at 10 m above the ground be averaged for at least 10 minutes, preferably 15–20 minutes, for use in any currently available predictive approach, and that comparison of predictions of spread rate be made with measurements also taken over a period of 15–20 minutes because accurately accounting for shorter term variation in spread caused by gusts and lulls and spatial variations in the fuel does not seem currently achievable.

As already noted, subdividing the firefront perimeter into small line segments (each of which is then propagated in the direction of the normal to the arc into unburned fuel, much as a straightline firefront would advance in accord with the quasi steady fire spread rate for the local fire environment) may result in overlap of the propagated arcs for regions of negative curvature. A physical basis pertinent to fire spread through discrete fuel elements is needed to guide "smoothing." Sethian (1996) categorizes the tracking of a set of marker particles to approximate the tracking of a moving front as a discretized Lagrangian approach. He suggests that a volume-of-fluid technique (Chorin, 1980) is an Eulerian approach (describing where the front is in terms of a fixed spatial grid), and probably superior. Only implementation can resolve questions of accuracy and feasibility for tracking a complicated firefront geometry by use of alternate discretized forms of Eq. (1). We question arbitrarily adopting changes to the propagation-speed function F to serve mathematical convenience. Osher and Sethian (1988) and Sethian (1996) suggest (by vague analogy, as if fire propagation were basically a hyperbolic phenomenon) that the fire-propagation function F be modified to the form $(F - \varepsilon\kappa)$, where ε is a small positive constant with the units of a diffusion coefficient and κ is the local curvature of the firefront; this modified form is amenable to so-called level-set methods, which still give rise to physically implausible cusps in the firefront evolution but do avoid mathematical multivaluedness. However, the only evidence (that fire propagation is related to firefront curvature) cited by these authors is a speculation by Markstein for flame propagation in homogeneous mixtures of reactive gases. Markstein (1964, pp. 21–23) addresses instances in which the radius

of flame curvature is comparable to flame-structure thickness because, under other circumstances, the role of curvature typically would be expected to be negligible (Carrier *et al.*, 1991). Markstein's speculation holds for phenomena in which classical diffusional processes in the direction of spread are essential to the mechanism of spread and in which the classical diffusional transport must be modified from planar representation to infer the correct rate of spread. Fire spread through chaparral-type surface fuels under wind aiding (diffusion-flame burning in a boundary layer of reactive vapor pyrolyzed from a condensed fuel) is not among such phenomena (see Section III.D). With respect to observations justifying the adoption of a curvature-dependent spread rate for fire propagation through surface-type fuels, Cheney and Sullivan (1997) do observe that if the head of a wind-aided grassfire remains narrow, the fire spread is slower than for a larger fire with a broad head. However, for a wind of 7 km/h, the effect of curvature on spread rate is negligible when the (say, maximum) width of the oval-configured perimeter of the wind-aided fire is 25 m; for a wind of 14 km/h, when the width is 100 m; for 21 km/h, 150 m; for very strong winds, about 200 m. There is a tendency for regions of the wind-aided-fire perimeter with large curvature to evolve to smaller curvature. Fires developing under strong hot winds increase their head-fire width quickly, and the time needed to attain the maximum rate of spread for the given fire environment (slope, loading, wind, etc.) is about 12 minutes (Cheney and Sullivan, 1997). The lesson is that significant effect of curvature on the quasi steady, one-dimensional spread rate is confined to a brief interval after ignition, and to a limited locale near the head under wind-aiding. The effect of curvature in general is insignificant for the practically interesting temporal and spatial scales of wind-aided fire spread pertinent to fire-fighting efforts. Furthermore, letting the fire-propagation function $F \rightarrow F[1 - j(\kappa)]$, where the function $j(\kappa)(< 1)$ monotonically decreases as κ decreases, may better express the limited field observations. If the wind ceased, aside from local effects at a large-curvature head, no inherent propensity toward a more circular perimeter from an established oval configuration is reported, to our knowledge; yet this is an implication of adopting the form $(F - \varepsilon\kappa)$ for vanishing F. In summary, the important geometric property derived from the flamefront configuration is the direction of the local normal vector pointing into the unburned medium. For any anomalous situation (in fire spread through a bed of fixed surface-fuel elements) in which the firefront curvature were to persist as a significant factor in firefront evolution, the simplistic formulation of Eq. (1) is probably inadequate to treat the phenomenon. If any such anomaly arises in an otherwise smooth evolution of the firefront configuration, physical judgment may well be a better basis for smoothing than any mathematical formalism, especially a formalism that creates implausible cusps and corners. With experience, an automated procedure for firefront propagation may be attained.

D. Closure of the Formulation for Fire Spread in Chaparral-Type Fuel Loading

The major challenge for implementing the semiempirical approach of Eq. (1) is to identify the dependence of the firefront-propagation-speed functional F on the environment-describing variables (for fire-spread-conducive, large-area-fire-generating conditions). We rewrite Eq. (1), which defines the firefront-perimeter velocity to be the local normal-to the-front advance rate, as $(i = 1, 2)$

$$\frac{\partial x_i}{\partial t} \equiv (V_f)_i = F(U, \theta; m, \ldots)v_i, \qquad x_i(\theta, 0) \text{ given} \tag{2}$$

where U denotes the (time-averaged) magnitude of the wind velocity; θ denotes the angle, measured counterclockwise, from the (time-averaged) direction of the ambient wind to the local outward normal to the firefront perimeter, v_i; m is the mass loading of thin fuel burned with firefront passage; and other parameters independent of U and θ may enter the argument of F. For simplicity, we deal here with a homogeneous fuel distribution with respect to type, thickness, height, and the like with a single simple ignition site, and with flat terrain, so that a value of θ uniquely defines a point on the firefront perimeter (Figure 6). Hence, we can dispense with the introduction of the parameter s. An interesting question is whether, under Eq. (2) and for a finite wind U, there exist translating, dilating, but geometrically self-similar firefront configurations. To answer this question, we should not write any approximation to Eq. (2) which involves F depending on anything other than a scalar function of U and θ. Discussion is limited to a homogeneous fuel bed of fixed properties and to no slope.

We now composite a very limited number of results for special values of θ, to constitute a smooth functional F applicable for all values of θ. We seek to formulate F so that, for a given fuel bed, the results from Eq. (2) agree locally with one-dimensional firefront-propagation rates known to hold for that fuel bed in each of three directions: the downwind direction $(\theta = 0)$, the upwind direction $(\theta = \pi)$, and the cross-wind direction $[(\theta = (\pi/2) \text{ and } (3\pi/2)]$. In fact, these "one-dimensional" rates are accessible from experiment (if executed) or modeling (if credible) but are currently at least partly unavailable. We now undertake to make plausible statements about spread in each of these three directions.

The peak rate of spread is in the downwind direction $(\theta = 0)$ (i.e., near site A in Figure 5). Accurately quantifying that rate is typically regarded to have highest priority in characterizing the functional F. In the downwind direction, conductive–convective heat transfer is the *dominant* mechanism that leads to fire spread; turbulent eddy transfer probably plays no important role in that part of the firefront perimeter. According to laboratory testing for *head-on* wind-

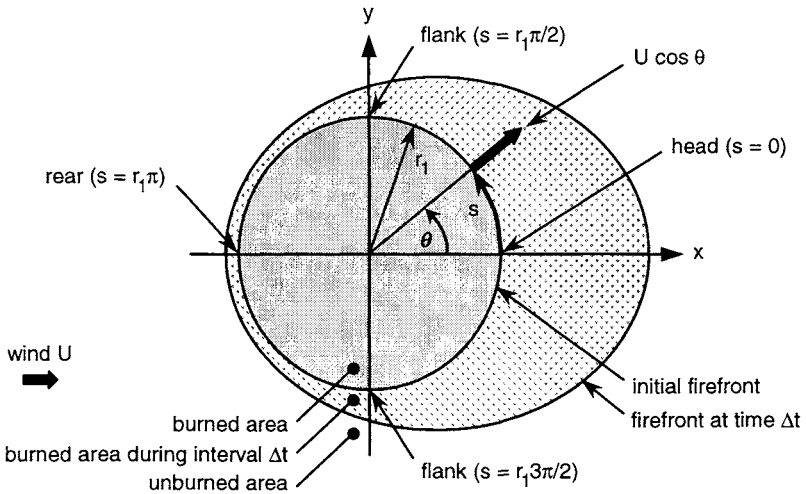

FIGURE 6 A particular example of the phenomena of Fig. 5, in which the initial perimeter of the burned area (at a time taken to be $t = 0$) is a circle of radius r_1. A wind of magnitude U arises at time $t = 0+$ and results in a head (where spread is with the wind), flanks (where spread is across the wind), and rear (where spread is against the wind). The fire spread during a time interval Δt (stippled area) results in the burned-area perimeter sketched at time Δt. The x axis, the primary ray for the angle θ, is taken to lie along the direction of the wind. If the wind changes direction to angle θ_1 with respect to the x axis, the revised Cartesian coordinates (x_1^*, x_2^*) of the point on the fire perimeter heretofore denoted (x_1, x_2) are identified by relations describing a simple rotational transformation of coordinates through angle θ_1; the x^* axis now is aligned with the wind, serves as the prime ray of the angle θ^* used in place of θ, and serves as the datum for the parametric distance s^* used in place of s.

aided fire spread across a dry uniform bed on flat terrain, $F(U, 0) \sim U^{1/2}/m^{1/2}$, where U is the speed of the head-on wind and m is (recalled to be) the dry thin-fuel loading (per unit planform area) burned during firefront passage (Wolff *et al.*, 1991); this result is shown to be consistent with the just-discussed mechanism for spread-sustaining heat transfer. Henceforth, we designate the functional $F(U, 0)$ by the symbol v_f. The expression ultimately must be modified because clearly there is a minimum loading for which fire spread does not occur, and clearly there may be a much reduced but perhaps still finite rate of spread as $U \to 0$. Nevertheless, the result is pertinent near site A. In Figure 5, we have taken the wind speed U to be constant in magnitude and direction over the spatial domain sketched, during the time interval $t_1 < t < t_2$, in accord with our simplified approach; we defer comment on the time averaging that would be required for so treating the wind encountered in a fire scenario.

At the flanks of the fire [$\theta = (\pi/2)$ or $(3\pi/2)$, e.g., near site B in Figure 5], the local normal component of the wind is zero, but the speed of propagation

is significantly larger than the speed for propagation under quiescent conditions. The firefront propagation is supported by (a) turbulent eddy transfer (lateral gusts) and possibly (b) the same mechanism that permits upwind transfer ($\theta = \pi$) (i.e., buoyancy-induced influx of fresh air down in the fuel bed) and somewhat localized radiative transfer among fuel elements in that bed. Much of the combustion may be of smoldering type. Cheney and Sullivan (1997) suggest that burning at the flanks alternates between heading fire and backing fire. Henceforth, we designate $F(U,|\pi/2|)$ by the symbol $\beta(U)$.

At site C in Figure 5 (i.e., at $\theta = \pi$), there is fire spread against the wind. This upwind propagation is attributed to mechanism (b) discussed in the last paragraph. The upwind propagation is here taken to be dependent on U since the airflow through the fuel bed competes with mechanism (b). For a fuel bed composed of discrete combustible fuel elements, Steward (1974, pp. 342, 372) suggests that the rate of fire spread directly against a wind U involves a balance of (1) radiative preheating and (2) convective cooling and finite-reaction-rate effects. Henceforth, we designate $F(U, \pi)$ by the symbol $\varepsilon(U)$. As a composite for F motivated by the discussion of phenomena at the three particular directions, we tentatively suggest ($\mu \approx 2-4$, as a first try):

$$F(U, \theta) = v_f(U \cos\theta) + \beta(U \sin^{\mu}\theta) \qquad \text{in } |\theta| < (\pi/2) \tag{3a}$$

$$F(U, \theta) = \beta(U \sin^{\mu}\theta) + \varepsilon(U \cos^2\theta) \qquad \text{in } |\theta| > (\pi/2) \tag{3b}$$

We expect, except possibly at very low values of U, that

$$\varepsilon(U) < \beta(U) < v_f(U) \tag{4}$$

In words, we expect the value of the spread rate F holding at the head ($\theta = 0$) to exceed the value of the spread rate holding at the flank [$\theta = (\pi/2)$ or $(3\pi/2)$], which, in turn, exceeds the value of the spread rate holding at the back ($\theta = \pi$).

At any given time, the locus of the firefront is given by

$$\left(\frac{\partial x_1}{\partial x_2}\right)_{t\ \text{const.}} = -\cot\left(\frac{\pi}{2} - \theta\right) = -\tan\theta \tag{5}$$

This equation is derived from trigonometric relations holding for the *tangent* to the firefront.

The firefront-tracking problem is obtained from trigonometric relations holding for the normal to the firefront, specifically,

$$\frac{\partial x_1}{\partial t} = F\cos\theta \tag{6}$$

$$\frac{\partial x_2}{\partial t} = F\sin\theta \tag{7}$$

with F given by Eq. (3), together with the constraint given by Eq. (5) and initial conditions giving the firefront locus at time $t = 0$: $x_1(\theta, 0)$, $x_2(\theta, 0)$. Numerically, Eqs. (6) and (7) may be used to advance the firefront perimeter over a brief interval of time Δt. From use of $x_1[\theta,(0), (\Delta t)]$ and $x_2[\theta(0), (\Delta t)]$ in Eq. (5), we obtain $\theta\{\Delta t; x_1[\theta(0), (\Delta t)], x_2[\theta(0), (\Delta t)]\}$. The cycle is then repeated: we obtain $x_1[\theta(\Delta t), 2(\Delta t)], x_2[\theta(\Delta t), 2(\Delta t)]$ from Eqs. (6) and (7), and then $\theta\{2(\Delta t); x_1[\theta(\Delta t), 2(\Delta t)], x_2[\theta(\Delta t), 2(\Delta t)]\}$ from Eq. (5). Of course, more sophisticated, iterative schemes for advancing the solution in time may also be used. A smooth interpolation for θ is needed, especially since the number of points on the firefront perimeter used to track the perimeter needs to increase as the perimeter becomes longer.

For explicitness, a possible trial form, consistent with Eqs. (3a) and (3b), is given by (for $\mu = 2$)

$$F(U, \theta) = \{\varepsilon_0 \cos^2\theta + c_1(U \cos\theta)^{1/2}\} + \{\varepsilon_0 \sin^2\theta + aU \sin^2\theta \exp[-bU \sin^2\theta]\}, \qquad |\theta| < (\pi/2) \tag{8}$$

$$F(U, \theta) = \{\varepsilon_0 \sin^2\theta + aU \sin^2\theta \exp[-bU \sin^2\theta]\} + \{\varepsilon_0 \cos^2\theta \exp[-\varepsilon_1 U \cos^2\theta]\}, \qquad |\theta| > (\pi/2) \tag{9}$$

This form for $F(U, \theta)$ implies that we have adopted the trial forms for the windspeed behavior at the head, flanks, and back to be

$$v_f(U) = \varepsilon_0 + c_1 U^{1/2}, \qquad \beta(U) = \varepsilon_0 + aU \exp(-bU), \qquad \varepsilon(U) = \varepsilon_0 \exp(-\varepsilon_1 U) \tag{10}$$

respectively. The parameters c_1, ε_0, ε_1, a, and b are independent of U and θ, but in general they depend on m, the mass loading of fuel, and other parameters characterizing the fuel bed. The parameters are anticipated to be so chosen so that, except for $U \to 0$, the ordering is $v_f(U) > \beta(U) > \varepsilon(U)$, in accord with Eq. (4). Marsden-Smedley and Catchpole (1995) characterize the spread rate at the flanks and back to be 40 and 10%, respectively, of the spread rate observed at the head of fires in Tasmanian buttongrass moorlands. Incidentally, Eqs. (8) and (9) give $F = \varepsilon_0$ at all θ for $U \to 0$: a circular perimeter remains circular as it expands through a uniform bed on flat terrain in the absence of wind. The form for v_f stems from the previously mentioned experiments by Wolff *et al.* (1991), although $\varepsilon_0 = 0$ in those experiments; the form for β, pertinent to the flanks, takes the variation of spread rate with wind speed to be nonmonotonic; the form for ε, pertinent to the back of the fire, takes the spread rate to be monotonically decreasing with increasing wind speed.

In Eq. (10), suppose we have a fuel bed for which: (1) $\varepsilon_0 = a = 0$ [no spread in the absence of wind, or at the flanks even with wind (Burrows *et al.*, 1991)], and (2) $v_f(U) = c_1 U^{1/2} H(U - U_{crit})$, where $H(x)$ is the Heaviside unit step func-

tion and U_{crit} denotes a finite minimal wind for the onset of spread under wind aiding (addressed in Section III.F). Then $F(U, \theta) = 0$ for $U < U_{crit}$; for $U > U_{crit}$,

$$\begin{aligned} F(U, \theta) &= c_1(U \cos \theta)^{1/2} \qquad \text{if } |\theta| < \cos^{-1}(U_{crit}/U) \\ \text{and } F(U, \theta) &= 0 \qquad\qquad\qquad \text{otherwise} \end{aligned} \tag{11}$$

According to the model, for a localized, pointlike ignition, we obtain a burned region confined within a wedge, with vertex at the ignition site, and with each arm of the wedge inclined at an angle $\cos^{-1}(U_{crit}/U)$ from the downwind direction. The burned region is only very roughly in the configuration of a sector of a circle because the firefront advance along the bisector of the wedge (i.e., in the direction of the wind) exceeds the firefront advance near the arms of the wedge. Experimental testing is needed to check this conjecture concerning the relation between (1) the finite minimal wind speed for flame spread onset after line ignition perpendicular to the wind direction, and (2) the configuration of the burn pattern emanating from the ignition of a single element in an equivalent fuel bed.

If we now generalize to a case in which the wind direction may vary in space and time, then we return to the use of the parametric length s of the firefront. At any time, the length s is measured from the initial ray $\theta = 0$, which is taken to be aligned with the wind direction at the moment of time under discussion. For a circular perimeter of radius r_1 at time $t = 0$ (Figure 6), with the x coordinate fixing the origin of the firefront length parameter s, the initial firefront is identified by

$$x_1(s, 0) = r_1 \cos \theta(s, 0) = r_1 \cos(s/r_1), \qquad x_2(s, 0) = r_1 \sin(s/r_1). \tag{12}$$

Thenceforth, from Eq. (1),

$$\frac{\partial x(s, t)}{\partial t} = [\cos \theta(s, t)]F, \qquad \frac{\partial y(s, t)}{\partial t} = [\sin \theta(s, t)]F \tag{13}$$

$$\tan \theta(s, t) = -\frac{[\partial x(s, t)/\partial s]_t}{[\partial y(s, t)/\partial s]_t} \tag{14}$$

where the subscript t signifies that time t is held constant in taking the derivative with respect to the length parameter s. This particular simple scenario would arise, for example, if there were an onset, at what we designate as time $t = 0$, of a wind U in what previously had been a point-ignited spread through uniform fuel on flat terrain under nil wind.

E. Coordination of an Experimental Program

The calibration/validation of the model might be initiated against historic data, but we suspect that any such data set is too incomplete for highly informative comparison of prediction with observation. Probably, comparison with historical fires ought to be complemented with comparisons with field tests involving prior inventorying and instrumentation. These field tests need not be carried out exclusively on the very large spatial scale that may be of ultimate interest; the algorithm may be usefully tested against relatively modest-scale fires under spread-aiding conditions. Indeed, once the model gains a modicum of credibility because its predictions compare favorably with observations, the model might be advantageously used in test planning. However, it seems doubtful that field testing would ever be approved for the very high fire-danger conditions for which a validated model seems most needed. Fire can propagate through chaparral at speeds up to about 3 m/s, with intensity of 10 MW/m of perimeter (Albini, 1984), whereas the typical upper limit for prescribed burning is roughly 0.5 MW/m of perimeter (Luke and McArthur, 1978).

Because the model is semiempirical in that information on the functional dependence of the local firefront-propagation speed on the key local state variables is taken to be input, extensive experimentation is required for model development, even prior to model calibration/validation.We have emphasized the importance of experimental results pertinent to the rate of fire spread at the head of a wind-aided fire, v_f, in formulating the more general expression pertinent to the rate of advance of the entire, often-closed firefront perimeter, F. To obtain an expression for v_f, we emphasize the suitability of quasi one-dimensional fire-spread experiments in which a quasi steady rate of spread is achieved (and measured) under *uniform* (and measured) conditions of slope, spread-aiding wind, and fuel-bed properties. In this paragraph, we address some considerations in carrying out such experiments. First, in the firefront frame of reference, a quasi steady rate of spread implies that a flaming zone of finite depth is propagating at constant speed, through a bed of sufficient length in the direction of propagation; a burned-over portion of fuel bed lies upwind of the currently burning zone, and a yet-to-be-burned portion of fuel bed lies downwind. At the very least, in the direction of firefront propagation, the upwind and downwind portions of the bed should be half as thick as the burning zone. The length of run to attain quasi steady spread increases with wind speed. Results in which the streamwise expanse of the flaming zone (i.e., the flame depth) increases with the length of travel (Anderson and Rothermel, 1965) may not have attained a quasi steady rate of spread. Also, departure from one-dimensionality is inevitably encountered at the lateral edges of the fuel bed, since downwind elements

are preheated from two sides in the core of the bed, but from only one side near the lateral edges of the layer. Thus, ideally, fuel beds of several different widths should be tested to establish that the spread rate taken to hold near the streamwise centerline of the fuel bed is a plausible approximation to that holding for an indefinitely wide bed (see Section IV.A). Such bed experiments are most conveniently initiated by simultaneously igniting the entire upwind edge of the fuel bed and tracking the continued progress (if any) of the firefront after the starting transient dies out and a constant rate of propagation is achieved. Further, it is preferable that experiments to obtain the rate of fire spread be conducted on the scale of physical interest. However, we repeat for emphasis: control to maintain constancy of the properties of the wind, fuel bed, and topography becomes more problematic in the field, and requirements on the amount and robustness of instrumentation increase. Because of limited control of conditions in large-scale experiments, reproduction of results is difficult to attempt, and even harder to achieve. Yet reproducibility seems essential for confidence that the key experimental parameters are clearly identified, and the observations of results are sufficiently accurate. Inevitably, the cost, difficulty, and turnaround time in experimentation increases as the scale increases, especially for spread under severe conditions; as a consequence, the desired fire spread data are most accessible on smaller scale (Carrier *et al.*, 1991; Wolff *et al.*, 1991; Weise, 1993; Catchpole *et al.*, 1998). The more limited opportunity for testing on larger scale is seemingly most advantageously used to confirm results already inferred from the smaller scale test data, or to modify the guidance drawn from the smaller scale test data owing to the role of phenomena (such as radiative transfer of heat, or even stratification of the atmosphere) that tend not to contribute prominently in smaller scale testing.

Though the rate of spread is the primary output for the intended application to flow-assisted fire spread, other quantities, such as suitably defined "flame height" and "flame tilt," may also be tabulated as functions of parameters characterizing key *prefire* properties of the environment (previously categorized as fuel-bed properties, meteorology, and topography). However, we do not emphasize relations among the spread rate, flame height, and flame tilt (e.g., Mongia *et al.*, 1998); such relations describe one unknown quantity in terms of another unknown and, by themselves, make a limited contribution. We do ascribe a significant role to analysis in assisting the selection of parameter values to be tested, and in the interpretation of data, especially if the melding of data taken on different scales to account for different contributing phenomena is entailed. For example, by modeling, we may be able to suggest tentatively, for validation or rejection by "one-dimensional fire spread testing," how to modify previously obtained, semiempirical results for the rate of spread on flat terrain, to incorporate the effect of a uniform positive (fire spread-assisting) slope in the direction of propagation. At the firefront, if we plot the vertical profile of the en-

thalpy (in excess of the ambient enthalpy) for the gas phase above the fuel bed, we may identify a characteristic height H for the profile. A positive slope of the terrain, δ, may imply a smaller value for H and, therefore, an enhanced characteristic heat-transfer rate from the hot gas to the portion of the fuel bed undergoing preheating to the pyrolysis-onset temperature (Fons, 1946). In fact, the enhanced heat-transfer rate owing to slope may be comparable to that for a higher spread-aiding wind speed U for a flat terrain with the same fuel bed. A simple theoretical analysis might give a strong indication in what functional form (whether an additive term or a multiplicative factor), involving which given parameters (in addition to δ, if any), to seek to summarize the data. Such a procedure ought to be more efficient than collecting data systematically for a large number of environment-describing parameters and then seeking formal correlations. On the other hand, we regard rapid fire spread modeling without close ties to testing to have little credibility.

Attempts to bypass this demanding agenda and to predict fire-growth rate across finite-element "parcels" by adopting conjectures about spread-rate "probabilities" without the aid of an extensive data base [as seen in the application of percolation theory to fire spread (Christensen *et al.*, 1993)] seem equivalent to guessing intuitively. One might just as well dispense with the probabilistic formalism and directly guess the firefront positions at future times. Without a basis for assigning probability densities, the probabilistic approach seems an arid formalism, and one might as well simply guess the answer immediately. Validation seems especially crucial for such an approach. Furthermore, "tuning" such an approach with data seems likely to be a highly inefficient utilization of the data, relative to the utilization of the data for upgrading more physically based approaches.

F. Contribution of Modeling to Data Correlation

A plethora of functional forms have been proposed for how rapidly the rate of fire spread v_f increases with the ambient wind speed U (Table 2); the literature contains even more perplexing results concerning whether the spread rate increases or decreases with increased thin-fuel loading (e.g., Cheney, 1981; Weber, 1991; Weber and de Mestre, 1991) (Table 3). For guidance in the interpretation of our own laboratory data for wind-aided fire spread across well-defined arrays of thin wooden fuel elements (Figure 7), we undertake a simple model and add complication only as a simpler theory proves inadequate to describe the observations. As a first trial, evolved from a suggestion by Taylor (1961), we take the rate of wind-aided spread to be that consistent with the known rate of entrainment of gas into the weakly buoyant, two-dimensional plume above a line source of heat (without associated release of mass or mo-

TABLE 3 Fire Spread Rate v_f Dependence on Initial Fuel Loading m ($v_f \sim m^p$)

Researcher	p exponent, m^p	Fuel type	Scale
Wolff *et al.* (1991)	-0.49^a	white pine toothpicks	lab
Cheney and Sullivan (1979)	0^a	grass	field
Rothermel (1972)	0^b	semi-empirical	lab; model
Burrows (1999a, 1999b)	0^a	jarrah litter	lab; field
Marsden-Smedley and Catchpole (1995)	0^a	buttongrass	field
Luke and McArthur (1991)	1^a	grass	field

[a]Data interpretation performed by the researchers themselves.
[b]Data interpretation performed by Gould (1991).

mentum). If we denote the strength of the line source (or fire intensity) by the symbol $\dot{Q}$, with units of heat per length (of line source) per time, then the proposal is that the speed of the cross-wind U and the characteristic speed of the buoyant updraft in the plume, W, are related by

$$U = 2\alpha W = 2\alpha[g\dot{Q}/(\alpha\rho_\infty c_p T_\infty)]^{1/3}$$

(see, e.g., Fleeter *et al.*, 1984). Here α denotes the dimensionless, empirical entrainment constant introduced by Taylor [$\alpha = O(0.1)$ for weakly buoyant

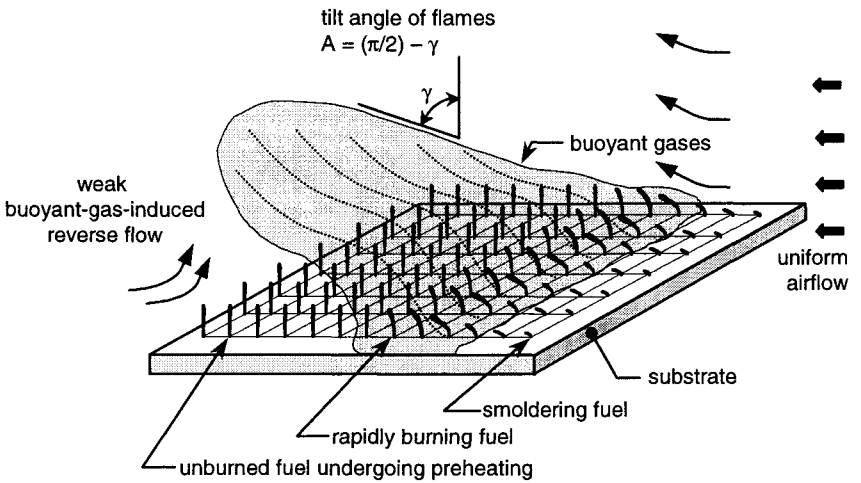

FIGURE 7 A schematic of the phenomenology of wind-aided fire spread across a bed of identical, upright, regularly arranged, thin, wooden fuel elements, supported in holes in an inert substrate. Artificial constraints are placed on the influx of air from the downwind side of the flamefront if, in the laboratory, wind is generated by drawing from downstream, rather than by blowing from upstream.

plumes, but α might be taken somewhat larger in order to apply the model to the highly entraining base of the plume]; g denotes gravity; c_p, the characteristic specific heat capacity at constant pressure of the gas (mainly air) in the plume; ρ_∞, the ambient density near ground level; and T_∞, the ambient temperature near ground level. If 2α is almost of order unity, we expect that, for $W > U$, a fairly vertical plume arises. However, for $U > W$, the conditions for our model to hold are not present, and we expect the plume to be more blown over. The flames then are inclined from vertical and typically extend downwind over the still-unburned portion of the fuel bed. The significance of the ratio $U^3/(50\dot{Q})$ (where U is in m/s and $\dot{Q}$ is in MW/m, and we have assigned the value $\alpha \approx 0.4$, as well as plausible values to the other factors) has been discussed for over a half century in the literature on local discharges in a cross-flow. If we take the speed of propagation of a line fire to be that associated with a steadily translating line source of heat, we write $\dot{Q} = \mathcal{Q}mv_f$, where $\mathcal{Q}$ denotes the effective chemical heat per mass of fuel burned, m denotes the mass (per unit planform area) of thin fuel burned during firefront passage, and v_f denotes the speed of fire spread. (For a given intensity $\dot{Q}$ of a propagating line fire, the quantities v_f and $m\mathcal{Q}$ are inversely related. However, the heat release rate per length of fireline, $\dot{Q}$, itself depends on fuel-preheating considerations, and thus possibly on $m\mathcal{Q}$.) By substitution for $\dot{Q}$ in the preceding expression for U, after rearrangement, $v_f \sim U^3/m$—a result well at odds with our laboratory results (Wolff *et al.*, 1991). We suspect that this first-try model is inadequate because a model based on weakly buoyant representation of processes in an above-fire plume omits the diffusive processes occurring in the flaming gas-phase boundary layer and in the fuel bed. However, for those previously discussed fuel beds for which fire spread is sustained only for wind speed above some finite threshold value U_{crit} (see the end of Section III.D), we may be able to use the plume-based model to estimate U_{crit}. It *may* be that

$$U_{crit} \approx 2\alpha[g\dot{Q}_{crit}/(\alpha\rho_\infty c_p T_\infty)]^{1/3}$$

In turn, we identify $\dot{Q}_{crit}$ by requiring that the flame length of a blown-over plume be of sufficient length to span the vegetation-bare ground between a burning hummock and its downwind neighbor, and thus to achieve contact ignition of the downwind neighbor. Typically, if the center-to-center distance between neighboring hummocks is denoted s, where $s \gg d$ (d being the diameter of a hummock), then, empirically, the flame length $L = p\dot{Q}^q$, where, for L in meters and $\dot{Q}$ in kW/m, $p \approx 0.15$ and $q \approx 0.4$ are typical values (e.g., Marsden-Smedley and Catchpole, 1995). Upon setting $L = s$ to identify $\dot{Q}_{crit}$, $U_{crit} \sim s^{5/6}$. Although the accuracy of the exponent is in doubt, U_{crit} increases as the distance between hummocks increases (Burrows *et al.*, 1991) because the updraft over a fire of greater intensity must be tilted to effect flame-contact ignition of the downwind neighbor. For small separation s, a fire of weak intensity suffices

to ignite the neighbor, and U_{crit} is small and may be equal to even zero: molecular heat-transfer mechanisms then may permit the flames temporarily supported by a burning element to ignite the neighbor, but such circumstances lie outside the focus of this discussion.

To relate the spread rate more accurately to wind and loading, in our next try we ignore gravitational effects. We develop a model in which the oncoming wind, heated by the gas-phase-diffusion-flame burning just above the already-pyrolyzing portion of the fuel bed, continues downwind to heat fresh unburned fuel from ambient temperature to the pyrolysis-onset temperature T_{pyr} to sustain the firefront propagation (Carrier *et al.*, 1991).

In the frame of reference of a steadily propagating firefront, we take the origin of coordinates to lie at the furthest-downwind site at which the fuel-bed surface is at the (known) pyrolysis temperature T_{pyr} (Figure 8). In such a frame, the fuel bed is translating upwind (in what we take to be the negative x direction) at a constant speed v_f. The ambient wind is flowing in the positive x direction at the constant known speed $(U - v_f) \approx U$, for cases of interest. We anticipate tentatively that the thin-fuel loading can be characterized adequately for present purposes by the overall quantity m, recalled to be the mass of thin combustible matter (per unit planform area of the bed) consumed with firefront passage. The fuel is sufficiently dry that moisture content is not a key consid-

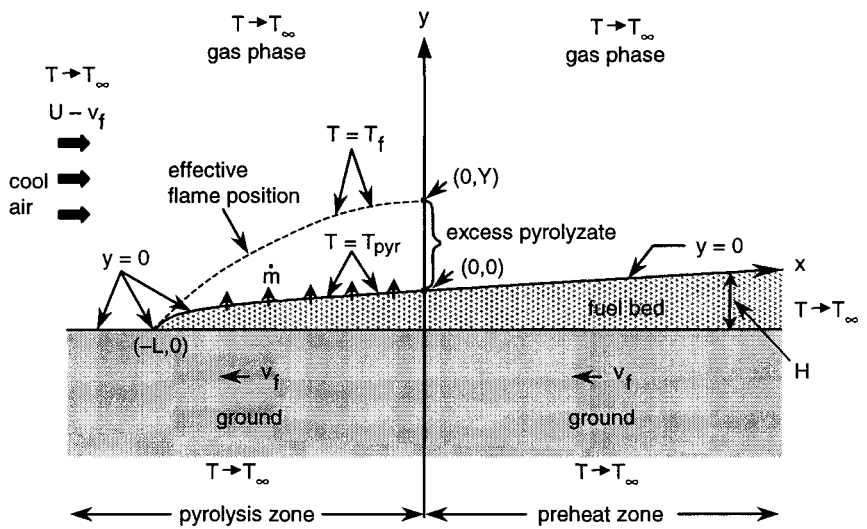

FIGURE 8 A simplistic idealization of wind-aided fire spread across a bed of discrete fuel elements, for the purpose of modeling a quasi steady spread at the rate v_f, typically (for the conditions of interest here) much slower than the speed $(U - v_f)$ of the ambient temperature oncoming air stream. The depiction is in the frame of reference of the firefront.

eration, and we tentatively ignore heat loss to inert content of the bed. Insofar as the portion of the thin fuel loading that burns with firefront passage is unknown prior to passage, we violate our dictum to relate v_f to parameters known prior to the fire passage. However, by using the total presence for the consumed loading m, we obtain a lower bound on the rate v_f (see discussion that follows). Furthermore, fires in grass and small shrub usually remove virtually all of the vegetation mass in the flaming combustion zone at the fire perimeter, and there is little if any smoldering residue after the flaming zone has passed, according to Albini (1992). More specifically, Minnich (1998, pp. 139, 147) characterizes chaparral fires as stand-replacement burns that denude most above-ground canopy owing to the high continuity and thinness of the fine fuels. There is scarce carryover fine fuels through burn cycles. On the other hand, Cheney and Sullivan (1997) suggest that head fires in Australian grasslands are somewhat less efficient and leave much of the lower fuel bed unburned. This is in marked contrast with prairie fires in the American Midwest, which typically leave very little unless the fuel is on the ground, and often not even then (P. Zedler, private communication).

We take all the heat derivable by combustion of the pyrolyzate (fuel vapor evolved from the polymeric loading m) to be released over the pyrolyzing surface of the fuel bed. "The flames of a wind-driven fire are more erect and often much taller at the front (i.e., head) than elsewhere on the perimeter" (Albini, 1992, p. 43). We ignore the fact that some of the combustible fuel vapor is not burned, or is burned (with ambient oxygen) downwind of the pyrolyzate-front position $x = 0$. Then, the conservation of energy per time per unit depth (perpendicular to the plane of Figure 9) is given by

$$v_f \mathcal{Q} m = \rho_0 c_p T_f U Y \tag{15}$$

where $v_f \mathcal{Q} m$ is recalled to be the intensity; $\mathcal{Q}$ denotes the net heat released by combustion per mass of vegetation; ρ_0 denotes the density of gas near the flame; T_f, the adiabatic flame temperature of the pyrolyzate/air diffusion flame; c_p, the specific heat capacity (at constant pressure) of the gas near the flame; and Y, the stand-off distance (at the pyrolysis-front position $x = 0$) from the surface of the fuel bed ($y = 0$) of the peak gas-phase temperature T_f. The value Y is an average, since Y varies on the integral scale of the turbulence. In Eq. (15) we are equating (1) the heat content per depth per time entering the gas phase from the pyrolyzing portion of the fuel bed and (2) the heat content (above ambient) per depth per time of the gas stream crossing the pyrolysis-front plane $x = 0$. The datum throughout this analysis is the ambient temperature, taken to be the same for the air and the bed, for convenience. We are ignoring any heating of the oncoming air stream (by a warmed substratum) upwind of the fuel-bed-burnout site, just as we are ignoring any gas-phase velocity-boundary-layer formation upwind of that burnout site.

The downward heat flux (in energy per area per time) from the gas phase

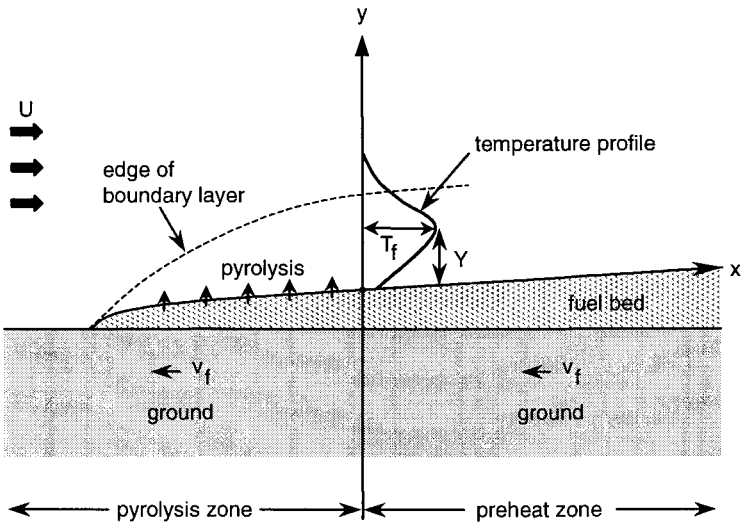

FIGURE 9 A schematic (supplementary to Fig. 8) in which it is emphasized that the diffusion-flame burning of pyrolyzate with ambient air occurs within the forced-convection boundary layer of the adopted model. The characteristic height of the maximum temperature T_f at the onset-of-pyrolysis front $x = 0$ is noted, along with a rough conjecture of the entire gas phase temperature profile at that streamwise position; the temperature approaches its ambient value at the edge of the boundary layer, and the onset-of-pyrolysis temperature at the fuel bed.

to the fuel bed over the preheating zone $\infty > x > 0$ (Figures 7 and 8) is expressed by

$$q = \frac{kT_f}{Y} f\left(\frac{x}{Y}\right) \tag{16}$$

where k denotes the thermal conductivity of the gas and the dimensionless function $f(x/Y) \to 0$ as its argument increases. This form implies that a convective-diffusive mechanism effects the preheating of fresh fuel from ambient temperature to pyrolysis temperature T_{pyr}. For later reference, were radiation (de Ris, 1979) the mechanism for preheating of fresh downwind fuel, if ε denotes the absorption coefficient of the hot gas and σ, the Stefan-Boltzmann constant, then, with Y again denoting the thickness of the hot layer,

$$q = Y\varepsilon\sigma T_f^4 g\left(\frac{x}{Y}\right) \tag{17}$$

where the dimensionless function $g(x/Y) \to 0$ as its argument increases. This behavior of $g(x/Y)$ is probably best envisioned for Y fixed and x becoming large.

For the heat balance within the fuel bed for the preheating zone, it is convenient (for this paragraph only) to reverse the sense of the coordinate axes, such that $\tilde{x}$ is positive upwind and $\tilde{y}$ is positive downward into the fuel bed;

$\tilde{x} = 0$ corresponds to that x at which the value of $f(x/Y)$ is effectively nil. Then, if subscripts $\tilde{y}$ and $\tilde{\xi}(\equiv \tilde{x}/Y)$ denote partial derivatives, and κ_b denotes the bulk thermal diffusivity of the fuel bed, the temperature (above ambient) in the preheating zone in the fuel bed is described by

$$\kappa_b T_{\tilde{y}\tilde{y}} - \frac{v_f}{Y} T_{\tilde{\xi}} = 0 \tag{18}$$

Any flow-associated transport of heat within the fuel bed is ignored. The Laplace-transform pair is recalled to be

$$\begin{aligned} \bar{h}(s) &= \int_0^\infty [\exp(-s\tilde{\xi})] h(\tilde{\xi})\, d\tilde{\xi}, \\ h(\tilde{\xi}) &= \frac{1}{2\pi i} \int_{-i\infty+\beta}^{i\infty+\beta} [\exp(s\tilde{\xi})] \bar{h}(s)\, ds \end{aligned} \tag{19}$$

where the real number β is chosen to be sufficiently large that all singularities lie to the left of $\mathrm{Re}(s) = \beta$ in the complex s plane. [Re(s) denotes the real part of the complex variable s.] Formally applying the transform to the temperature-field equation and then solving under the condition of boundedness (for a fuel bed approximated, for this manipulation only, to be of semiinfinite depth, for simplicity of expression) yields, if $A(s)$ denotes a function of integration to be identified,

$$\bar{T}(\tilde{y}, s) = A(s) \exp\left[-\left(\frac{v_f s}{\kappa_b Y} \right)^{1/2} \tilde{y} \right] \tag{20}$$

When q is expressed as a function of $\tilde{x}$, it is denoted $\tilde{q}$; when f is expressed as a function of $\tilde{x}/Y$, it is denoted $\tilde{f}$. Application of the boundary condition for convective-diffusive preheating gives, after use of the Laplace transform,

$$\bar{\tilde{q}}(s) = \frac{kT_f}{Y} \bar{\tilde{f}}(s) = -k_b \bar{T}_{\tilde{y}}(0, s) = k_b \left(\frac{v_f s}{\kappa_b Y} \right)^{1/2} A(s) \tag{21}$$

Therefore,

$$\bar{T}(0, s) = A(s) = \frac{k}{k_b} T_f \left(\frac{\kappa_b}{v_f Y} \right)^{1/2} \frac{\bar{\tilde{f}}(s)}{s^{1/2}} \tag{22}$$

At the pyrolysis front, $\tilde{\xi} = \tilde{\xi}_{pyr}$ at the interface $\tilde{y} = 0$, upon inversion of the transform,

$$T_{pyr} = \frac{k}{k_b} T_f \left(\frac{\kappa_b}{v_f Y} \right)^{1/2} N, \qquad \text{where } N \equiv \frac{1}{2\pi i} \int_{-i\infty+\beta}^{i\infty+\beta} \frac{\bar{\tilde{f}}(s)}{s^{1/2}} \exp(s\tilde{\xi}_{pyr})\, ds \tag{23}$$

that is, N is just a dimensionless positive real number whose value depends on details (of the heat-transfer profile) that we do not specify (because we believe that such matters will remain accessible only by experiment for a long time into the future). If Eq. (16) is solved for Y and substituted in Eq. (23), we obtain, if $\kappa_b \equiv k_b/(\rho_b c_b)$,

$$\frac{v_f}{U} = N\left(\frac{k\rho_o c_p}{k_b \rho_b c_b}\right)^{1/2}\left(\frac{T_f}{T_{pyr}}\right)\left(\frac{kT_f}{QmU}\right)^{1/2} \tag{24}$$

The dependence on the square root of the ratio of the so-called conductance for the gas phase to that for the "solid phase" is conventional in such phenomena; we regard the product $k_b\rho_b c_b$ as a *composite property* of the bed and do not regard it as appropriate to attempt an approximate evaluation of any one factor in terms of other quantities that have been introduced. The appearance of the product Qm indicates that it is the net obtainable exothermicity (per unit planform area of the fuel bed) that is significant for the spread rate.

The presentation of Eq. (24) is nondimensional, but in practice no factor other than m and U is easily varied appreciably (Albini, 1992). The relation $v_f \sim (U/m)^{1/2}$ can hold *over only a limited range of parametric values,* since we expect that (1) other processes permit finite (if slow) rates of spread in the absence of wind, or against the wind; (2) sufficiently high wind could result in forced-convective extinction of thin fuel elements; and (3) nonpropagation may occur for either sufficiently sparse loading (because an upwind element may burn out without preheating its downwind neighbor to its onset-of-pyrolysis temperature) or sufficiently dense loading (because of oxygen deprivation within the bed, or radiative heat loss from thick fuel elements). In short, many finite-rate processes not accounted for in the foregoing continuum-like treatment of the fuel bed may enter, so only experiment can confirm for what (if any) thin-element loading and ambient wind speed this model holds. Of course, we would not have included this convective/diffusive-preheating development without experimental verification (Wolff *et al.*, 1991) that $v_f \sim (U/m)^{1/2}$ holds for a toothpick-type fuel bed with $0.0 < U < 4.6$ m/s, 0.11 kg/m$^2 < m < 0.88$ kg/m^2, so $0 < (U/m) < 40$ m^3/(kg s).

Indeed, we just briefly note that the corresponding radiative-preheating development, in which we adopt Eq. (17) in place of Eq. (16) and obtain [M is a dimensionless positive real number with value related to the here-unspecified details of the profile $g(x/Y)$]

$$\frac{v_f}{U} = \left(\frac{\rho_o c_p T_f}{mQ}\right)^{3/2}\left(\frac{T_{pyr}}{T_f}\right)\frac{(\rho_b k_b c_b U)^{1/2}}{M\varepsilon\sigma T_f^3} \tag{25}$$

The brevity of this discussion stems from our not having observed this result in our testing. We believe (Carrier *et al.*, 1991) that this result [i.e.,

$v_f \sim (U/m)^{3/2}$] *might* be observed for an exceptionally heavy fuel loading, say, $m = O(2\ \mathrm{g/cm^2})$.

Williams (1977) notes that the rate of quasi steady, one-dimensional spread of fire through a combustible medium is often usefully discussed by adopting a firefront structure in which there is a nonflaming ("preheat") zone, within which, continually, fresh fuel is warmed from ambient temperature to ignition temperature:

$$\rho_b v_f h_i = I, \qquad \text{where } h_i = c_b T_i \tag{26}$$

and it is recalled that the datum for temperature is the ambient temperature; I, with units of heat per area (perpendicular to the direction of propagation) per time, denotes the flux furnished to the fresh fuel by convection, conduction, and/or radiation from the flaming region (not encompassed within this examination, which is limited to a *subdomain* of the complete firefront structure). The ignition temperature T_i may be *roughly* identified with the onset-of-*vigorous*-pyrolysis temperature T_{pyr} for the vegetation of interest (Albini, 1992). Williams (1977) points out that this one-dimensional treatment is *not* readily applied to scenarios in which a fuel bed yields pyrolyzate (burned in the gas phase above the bed), as the fuel-bed surface regresses in a direction perpendicular to the direction of propagation. Indeed, Frandsen (1971) notes the inherent two-dimensionality of fire spread over a fuel bed (especially wind-aided fire spread) by emphasizing the need to supplement the heat flux (to fresh fuel) in the direction of propagation with a contribution involving the heat flux (to fresh fuel) perpendicular to the direction of propagation.

Pyne *et al.* (1996, p. 37) write: "Rothermel's fire spread model (1972) is the basis for most computer-based fire management applications in the United States, with significant use in other countries. . . . Rothermel's model was developed from a strong theoretical base in order to make its application as wide as possible. This base was provided by Frandsen (1971) who applied the conservation of energy principle to a unit volume of fuel ahead of an advancing fire in a homogeneous fuel bed. In his analysis, the fuel-reaction zone is viewed as fixed and the unit volume moves as a constant depth toward the interface. The unit volume ignites at the interface. Rate of spread is then a ratio between the heat received from the source and the heat required for ignition by the potential fuel. Frandsen's equation . . . contained heat flux terms for which the mechanisms of heat transfer were unknown. To solve the equation, it was necessary to use experimental [data]." Since Rothermel's model is widely used (Andrews, 1991), we consider the model in detail. We have our reservations about seeking universality in semiempirical models. Also, we question the citation of Frandsen's work as a basis for Rothermel's model, which is in the category of one-dimensional models typified by Eq. (26); the just-described model [Eqs. (15)–(25)] explicitly encompasses the role of heat transfer transverse to the direction

of propagation, and perhaps better includes the processes thought essential by Frandsen. [Incidentally, the multidimensional treatment of firefront advance traces to work by Thomas and Simms in 1963, as Frandsen (1971) himself acknowledges.] One-dimensional models for fire spread through wildland vegetation were state-of-the-art when discussed by Emmons (1963, 1965), but multidimensional treatments of spread have now been undertaken. Further, in his one-dimensional modeling, Emmons treated the flaming zone and bed burnout, as well as the preheat zone, and adopted an explicit, radiative mechanism for the preheating of fresh fuel. We are able to discern a treatment of preheating, but no clear treatment of the rest of the firefront structure, in the Rothermel model. Indeed, Albini (1984, p. 594), in discussing the genesis of Rothermel's model, writes, "the pivotal step in the development of the model was [an] inspired conjecture." Specifically, Rothermel takes (Pyne *et al.*, 1996), in terms of the notation adopted earlier, and with ξ denoting the fraction of the product $m\mathcal{Q}\Gamma$ that serves to preheat fresh fuel to ignition (so propagation may continue),

$$I = m\mathcal{Q}\Gamma\xi(1 + \phi_s + \phi_w) \tag{27}$$

where the factor Γ is termed a velocity by Rothermel (though it has the units of a frequency), and ϕ_s and ϕ_w are dimensionless empirical expressions giving the increment to the fire spread rate owing to finite slope and finite wind, respectively. Although a great variety of functional forms can be fitted to a limited amount of data, we know of no analysis that motivates adopting the form of Eq. (27) for the quantity I. Whether the model is based around convection and/or diffusion and/or radiation, as the primary mechanism of preheating of fresh fuel, is not explicit. We are left uninformed about the basis of taking the effects of slope and wind on spread rate to be additive and effectively independent (Mongia *et al.*, 1998). By inspection, Eq. (27) requires that fire propagate in a situation without wind or slope, if wind or slope are to augment the spread rate—a requirement for which counterexamples are readily demonstrated (e.g., Burrows *et al.*, 1991). In fact, taking ϕ_w to be an additive contribution, universally proportional to a power of the wind speed U, precludes encompassing cases in which there is an abrupt increase of spread rate above a threshold wind, then a modest increment with further increase of wind speed (Gill *et al.*, 1995). Further, in the Rothermel model, the rate Γ is taken to be primarily an empirical function of (besides m) the (true) density of the vegetative matter, fuel-bed depth, the ratio of surface area to volume of fuel particles, fuel mineral content, and fuel moisture content; fuel availability is related empirically to moisture content only. But could not elevation of the fuel bed (ambient pressure), diffusional and advective processes within the vegetative matter and in the gaseous interstices, and chemical kinetics play a comparably important role in the rate Γ? Because the forms adopted for Γ, ϕ_s, and ϕ_w are curve fits which give v_f correctly for the available data, but for which even the simplistic, primitive moti-

vation that went into Eqs. (15)–(25) is lacking, it would seem crucial that the model be validated against a wider data base than was used in its formulation. The model was distributed and in wide use before this validation was performed; shortcomings of the model and the need for revision have since become apparent (Albini, 1984). Perhaps the spread rate v_f, for use in forming the functional F in Eq. (1), might be best ascertained by proceeding with both testing and modeling from scratch, and regarding the Rothermel model as a historic milestone. There are likely to be several other attempts to be abandoned [perhaps including Eqs. (15)–(25)] before an adequate statement of the dependence of the spread rate v_f on prefire parameter values is in hand.

IV. PRELIMINARY TESTING OF THE MODEL

About 200 experiments on wind-aided fire spread across a well-defined, horizontally oriented array of very small diameter (1.3–4.4 mm), discrete fuel elements were carried out in the previously described, specially designed and dedicated firetunnel. This experimental setup allowed investigation of factors such as fuel-bed width, fuel arrangement, inert content, moisture, and substratum. Of course, it is the thin fuels that are burned exothermically with firefront passage. These thin fuels are quickly responsive to changes in moisture/heat and most readily combustible. Post-firefront combustion of some of the thicker fuel has relatively little bearing on the speed of the firefront advance.

A. Fuel-Bed Width

A curved firefront evolves from ignition along a straight line perpendicular to the direction of the oncoming wind, owing to the fact that, at a given distance downwind, those fuel elements situated near the lateral edges of a finite-width bed are less effectively preheated by the approaching, upwind firefront than the fuel elements situated in the interior of the bed (i.e., further from the edges). The retardation in the rate of fire spread is manifested further and further from the lateral edges with increasing downwind distance, so eventually a curvature characterizes the entire firefront of any finite-width fuel bed (Figure 10). We have noted that only the component of the oncoming wind that is locally normal to the firefront aids spread; once the flanks lag, they continue to lag. Inserting structures at the lateral edges of the bed cannot replicate the perfectly noncatalytic, perfectly slippery, perfectly adiabatic conditions holding for a perfectly one-dimensional fire spread; ascertaining the consequences of adding physically realizable constraints at the lateral edges (Catchpole *et al.*, 1998, Figure 3) is problematic. Investigating the consequences on fire spread rate of increasing

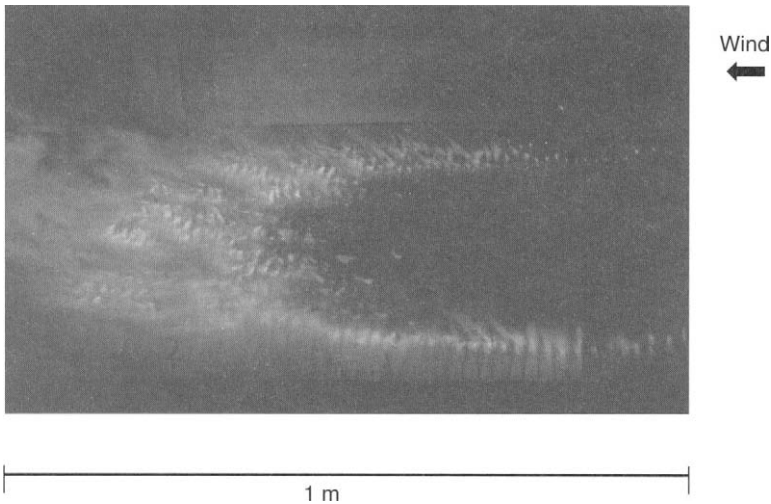

FIGURE 10 A photograph of the firefront curvature for wind-aided fire spread across a bed of vertical white-pine toothpicks. Here, the fuel loading $m = 0.11$ kg/m^2, the wind speed $U = 1.6$ m/s, and the fuel-bed width $W = 1.0$ m. The site is roughly 2 m downwind from the leading edge of the fuel bed, where the firefront was initiated along a straight line.

the bed width in the hope of extrapolating the spread rate to the value holding for an indefinitely wide bed is probably not feasible for most facilities. Furthermore, it may be important to consider that, as tests are executed for successively wider fuel beds within a test section of fixed width, some oncoming air, diverted around a "heat island" for a fire spread test with a narrower bed centered in the test-section, may be constrained to more two-dimensional streaming for a wider bed which approaches the test-section width of the facility. The upshot is that spread rate may be dependent on the width of the facility as well as on the width of the fuel bed. The information that seems accessible is the comparison of how spread rate varies with fuel loading, wind speed, and the like for a fixed bed width within a given facility.

B. Fuel Arrangement

To avoid meticulous and tedious inventorying of fuel, one hopes that the fire spread rate can be characterized by a single parameter, the fuel loading m, as long as the fuel elements are wooden, "thin" [less than ~0.3–0.6 cm in thickness (Cheney, 1981; Albini, 1992), so the elements remain isothermal under gradual heating], and upright. Then, recording the fuel mass before and after flaming-firefront passage is simplified, since we have noted that virtually all the

fuel is consumed. Testing with well-defined fuel beds facilitates reproduction of test conditions to establish error bounds. For toothpicklike fuel elements [of density ρ_s, (exposed) height H, and characteristic cross-sectional area d^2] inserted upright into regularly distributed holes (drilled into a substrate), the fuel loading m is given by [$(1 - \phi)$ is defined as the packing ratio and $\rho_s(1 - \phi)$, the bulk density]

$$m = \rho_s H(1 - \phi) = \rho_s H(nd^2) = \rho_s H(Nd^2/s^2) \tag{28}$$

The porosity (voidage) ϕ is varied to change the fuel loading m; more specifically, the number of fuel elements per unit area of the bed, n, is varied—where $n = N/s^2$, with N denoting the number of fuel elements (however distributed) in an area s^2, where the distance s characterizes the square-grid spacing. For heavier loading, we may insert many toothpicks in a given drilled hole; for lighter loading, we may leave many holes unoccupied. If we further fix n for a single-height constant-cross-sectional-area fuel-element type, then only small-scale variability is possible within a fuel bed of a given loading. The basic "building block" is the smallest square delineated by four drilled holes; the square (conveniently taken with one side parallel to the leading edge of the fuel bed) is meticulously repeated to comprise the entire array for the tests. For example, one can obtain an average of one toothpick in each hole by placing two toothpicks in every other hole. The presence of more than one toothpick per hole augments the possibility of shading one fuel element from some radiation owing to the presence of another. For more complicated arrays, with mixed elements, a larger basic building block is used. While [for fixed wind speed, fixed fuel-loading parameters (ρ_s, H, n, d^2), and fixed bed width] some variability of the rate of fire spread, especially for lighter loadings, is observed, *still, our preliminary testing shows that the rate of spread may be described usefully in terms of the macroscopic description m.* For example, Figure 11 shows the sensitivity of the rate of fire spread to microscale details, for the case in which there is the equivalent of two white-pine toothpicks per hole. What little sensitivity there is, is owing to a slightly faster propagation for those arrangements in which a downwind fuel element is closer to an upwind element, with both oblique and in-line considerations of importance. Incidentally, we regard the value of the fuel density ρ_s as effectively invariant for cases of interest.

However, because so simplistic a treatment of the fuel bed may be adopted inappropriately, in the rest of this subsection we dwell at length on circumstances that render the one-parameter characterization unsuitable. For example, we have yet to discuss the consequences of altering H and/or d (within the constraints of a "thin" fuel); these matters are examined in Section V. Cheney and Sullivan (1997, p. 25) write, "Fuel load by itself does not influence rate of spread of grassfires. While previous publications have reported that fuel load directly influences a fire's rate of spread, we have found that this occurs in grass-

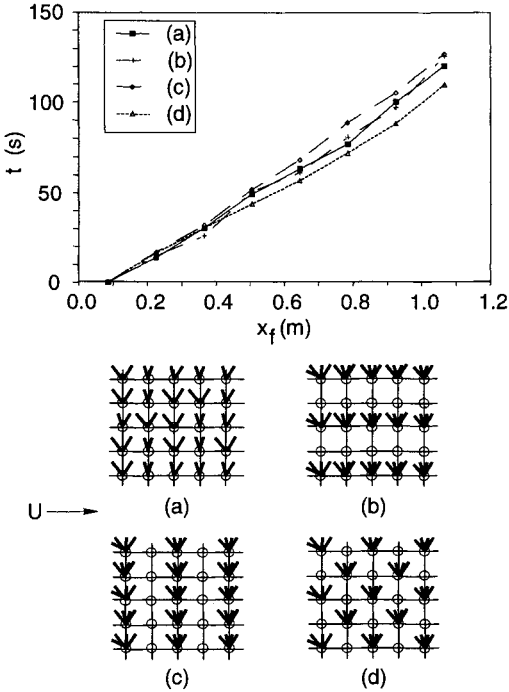

FIGURE 11 Effect of the fuel-loading pattern on the rate of firefront propagation v_f for fuel loading $m = 0.88$ kg/m^2, test-bed width $W = 0.55$ m, and wind speed $U = 0.7$ m/s. The quantity x_f is the streamwise centerline position of the firefront (downwind from the leading edge of the fuel bed), and t is the time since ignition. The hole-center-to-hole-center spacing is 1.25 cm.

lands only if changes in fuel load also reflect changes in fuel condition, in particular changes in fuel continuity." Of course, all fuel beds of interest in a wildland-fire context consist of discrete combustible elements; those fuel arrays described by Cheney and Sullivan (1997) as "continuous" have relatively small separation distance s: if oxygen is accessible, a finite (but, for our purposes, typically very low) rate of fire spread may be sustained even in the absence of wind. Cheney and Sullivan (1997, pp. 24–25) report that, in grasslands typified by upright stalks (and presumably comparable values of ρ_s), the rate of spread is largely independent of the values of m (the loading), H (the bed height), and Nd^2 (the fineness of the stalks) but is quite sensitive to the value of s (the "continuity"); *if* all the thin fuel burned with firefront passage, so that m were identical with the initial fuel loading, then, in view of Eq. (28), these statements are inconsistent. (See also their Fig. 4.15 on p. 32.) Cheney and Sullivan seem to suggest that the graininess (patchiness) of a discrete-fuel distribution may be

so pronounced that the convenient single continuum descriptor m is insufficient for fire spread rate characterization, and one must revert to description of the fuel in terms of multiple constituent factors such as H and s, perhaps even taking account of the variation of properties with height within the bed. Circumstances in which such detail is essential to fuel-bed description for fire spread prediction undoubtedly arise. However, the fact that Mediterranean garrigue or Australian mallee may be so discontinuously distributed that sustained fire spread is likely only under strong surface winds does not in itself ensure that the single descriptor m is not useful for fire spread rate estimation. For an example discussed by Cheney and Sullivan, some grassland in the arid center of Australia consists of combustible dense clumps (spinifex hummocks) and bare interstices, both of roughly 1-m lateral scale, so the interstices serve as firebreaks, except under high wind that abets otherwise precluded fire spread. Perhaps the closest American analogue is sagebrush, an upright aromatic shrub with narrow grey leaves. Sagebrush grows to a height of about 0.5–3.5 m on semidesert plateau between the Rocky Mountains and Pacific Ocean. The patchy vegetation supports fire spread only under high wind. Another American analogue is the grass tussocks on the northern-Alaska tundra. Characterizing spinifex hummock grassland in terms of the single parameter m, even if in general inadequate for characterizing fire spread rate, may suffice for the special *subset* of conditions pertinent to relatively rapid fire spread. In fact, Gill *et al.* (1995, pp. 31–32, including Figure 6) state, "When the wind is above the threshold for spread, the fire may spread at the same rate as in continuous fuel"—so characterization of the surface-fuel bed in terms of m for fire spread rate estimation may be no more or no less appropriate at *any finite* rate of spread, independently of the value of s. Incidentally, Gill *et al.* (1995, pp. 32–33) discuss the frustration in using formulae for spread rate inferred from data obtained in one series of field experiments on hummock grassland to predict the fire spread rate in another series; such experience suggests that a useful contribution may be more accessible through reproducible testing under well-defined, well-controlled conditions in the laboratory (Section II). We reiterate that our primary focus is on fire spread in high-continuity, thermally thin fuels such as the dense, carpet-like, mature stands of chaparral in southern California for which graininess (coarseness of the fuel distribution) is often not as prominent a consideration.

Cheney and Sullivan (1997) find that the rate of fire spread is independent of the initial total thin-fuel loading (prior to firefront passage), but is highly sensitive to (1) the curing state of a grassland, expressed as the fraction of dead material in the sward, and (2) the drying out of the dead grasses. Specifically, the rate of spread is nil for a curing state below 50% and increases monotonically and significantly with curing state above 50%; the rate of spread is often nil for fuel-moisture content above 20% of ovendry weight and increases monotonically and significantly for lower moisture content. If we recall that the parame-

ter m refers to the loading of thin fuel *burned during firefront passage* (Section III.D), sometimes termed the "available" thin-fuel loading, then perhaps we narrow the apparent discrepancy between field and laboratory observations with respect to the dependency of the rate of spread on the amount of fuel. We recall (Section III.F) that Albini (1992) comments that virtually all thin fuel typically is burned during firefront passage in grass and small shrub; Minnich (1998) notes that such completeness of burns holds for chaparral in southern California. Burrows *et al.* (1991, pp. 196, 198) state that fire spread in spinifex entails complete burning of all above-ground parts of the plant in the flaming zone, though they confuse the issue by also discussing flaming hummocks behind the main head fire. However, Cheney and Sullivan (1997) found that fast-spreading grass fires left appreciable thin fuel unburned in Australian field tests. Marsden-Smedley and Catchpole (1995) make the same observation concerning fire spread in Tasmanian buttongrass moorlands. Accurate prediction, over the range of fire spread conditions, of the available (as distinct from the total) thin-fuel loading is sometimes challenging. Unfortunately, the rate of fire spread may be related to a quantity which, while a convenient gross descriptor, is not always known prior to firefront passage.

Laboratory experiments with poorly reproducible fuel beds (Burrows, 1999a, 1999b) result not only in large scatter in the spread-rate data but also in no clarification of the spread-rate dependence on available fuel.

C. Inert Content

The presence of noncombustible material in the fuel bed (effectively including higher moisture-content, thicker fuel that does not burn with firefront passage) may introduce heat-sink and/or wind-retardation effects. When the inert material is well-mixed with combustible polymers, an oxygen-deprivation effect may also arise, so that vigorous burning is inhibited and copious smoke may be produced. This oxygen-deprivation effect is not readily investigated with the upright-fuel-element/upright-inert-element arrangement adopted here for examination. We consider fuel beds in which finishing nails are regularly distributed (12.8 kg/m^2) (Figure 12), in the midspan only, for three tests (Figure 13) in which the discrete fuel elements are white-pine toothpicks (0.22 kg/m^2). Both upwind and downwind of the midspan, the white-pine fuel loading is identical to that of the midspan, but no nails are present. Figures 14 and 15 present the results of other tests with nails present; the inserts symbolize the loading of the midspan, with a left-leaning mark denoting a nail-filled hole in the substrate, a right-leaning mark denoting a toothpick-filled hole, and a small dot with no mark denoting an empty hole. We define R to be the ratio of the number of nails to the number of toothpicks.

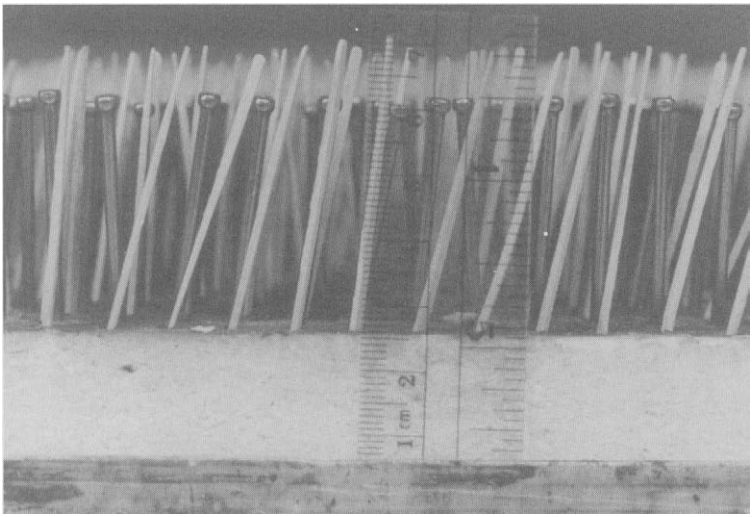

FIGURE 12 A side view of the midspan (of a pretest fuel bed) consisting of common nails interspersed regularly amid white-pine toothpicks.

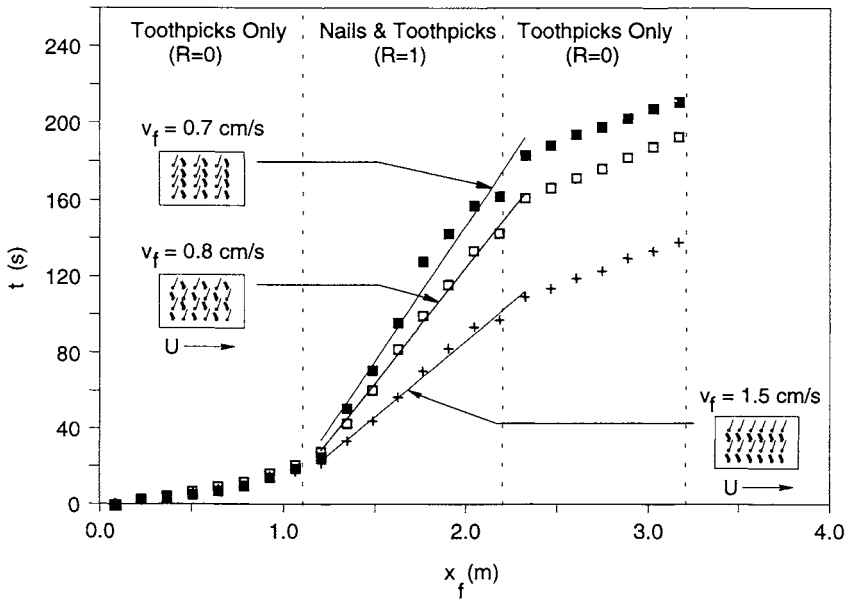

FIGURE 13 The firefront position x_f vs. time t for tests conducted with white-pine toothpicks at a fuel loading $m = 0.22$ kg/m^2, a wind speed $U = 2.5$ m/s, and a fuel-bed width $W = 0.55$ m. The ratio R (the number of nails divided by the number of toothpicks) is unity for the midspan of the fuel bed and zero elsewhere. The inset depicts the nail-and-toothpick arrangement in the midspan, where left-leaning lines represent nails and right-leaning lines represent toothpicks.

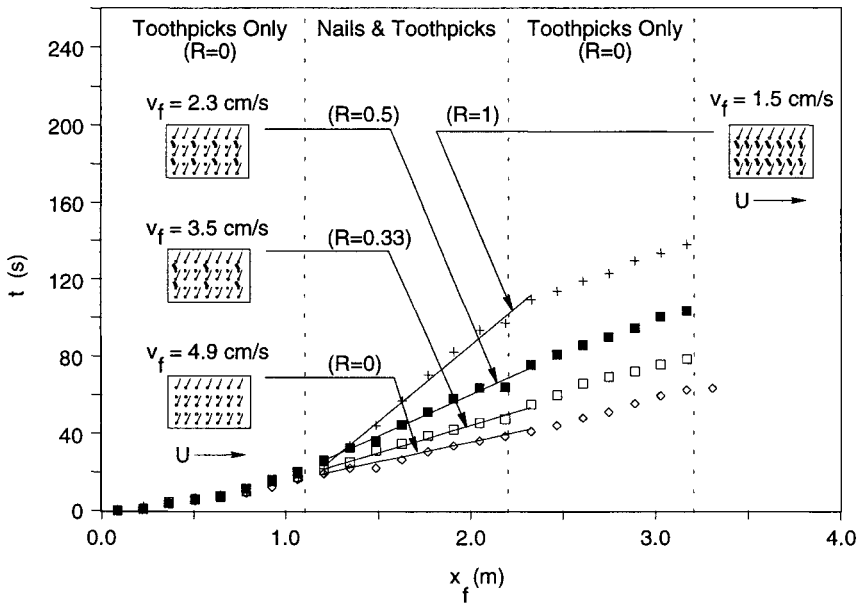

FIGURE 14 Same as Fig. 13, except the ratio R takes on the successive values, 0, 0.33, 0.50, and 1.0 (for the midspan only) for the four cases tested. In the inset, a dot without a line denotes an empty hole in the substratum.

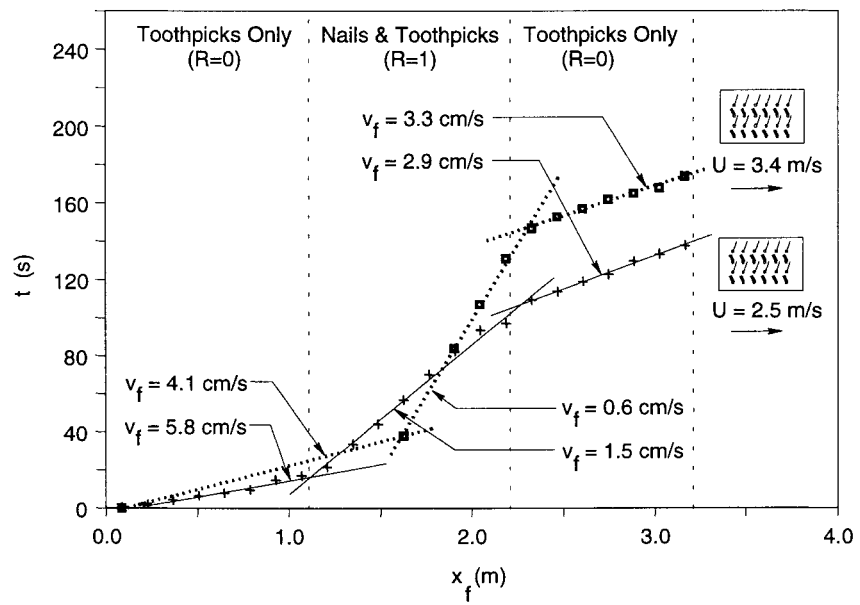

FIGURE 15 Same as Fig. 13, but with the ratio $R = 1$ for two tests with different wind speeds, $U = 2.5$ m/s and $U = 3.4$ m/s.

Figure 13 illustrates that the pattern of loading of inert material alters the fire spread rate, even for fixed total amount of combustible and inert material. The ratio R in the midspan is unity in all three tests shown, but the rates of fire spread differ by a factor of two in the midspan. The preheating capacity of a burning fuel element is strongest on a neighbor located immediately downwind; if that neighbor is an inert nail, the fire spread is slowed. Therefore, for these tests, the arrangement of the fuel has an effect on the resulting fire spread rate, and the fuel bed cannot be characterized by a single loading value, as indicated earlier for an arrangement of upright combustible elements only.

Figure 14 presents results for $R = 0, 0.33, 0.5$, and 1, with m and U held constant; v_f decreases monotonically as R increases. Increasing the amount of inert material in the bed significantly reduces the fire spread rate. The relative importance of (1) the heat-sink effect and (2) the wind-retardation drag (so the effective wind speed U is reduced), owing to the presence of the nails in the midspan, is uncertain.

In Figure 15, the spread rate v_f decreases in the midspan (where nails are present) when the wind speed U is increased from 2.5 to 3.4 m/s, whereas an increase in wind speed increases the spread rate in the nail-free regions. The observed behavior in the midsection may be evidence of a so-called finite-Damköhler-number effect in fire spread across discrete fuel elements, where the Damköhler number D_1 is defined to be the ratio of a characteristic reaction rate to a characteristic flow rate. For D_1 sufficiently small, the chemical reaction is extinguished ("chemically frozen" flow); if D_1 is sufficiently large, the chemical reaction proceeds at chemical-equilibrium rates; for intermediate values of D_1, transport rates and reaction rates are competitive, and a faster flow implies a slower rate of chemical reaction. Upwind and downwind, presumably D_1 is sufficiently large for the flow to be in chemical equilibrium; the faster flow is responsible for a faster rate of spread under rate-of-preheating-controlled considerations. In the midsection, the temperature may be reduced owing to the presence of a heat sink (the nails), and the chemical-reaction rate typically decreases exponentially as the temperature is reduced. Rather than being under preheating-mechanism control, the spread rate is under reaction-rate control, and an enhanced wind speed implies a reduced spread rate.

The presence of effectively noncombustible material seems typically not a major issue in the chaparral context of primary interest.

D. Moisture

The ambient moisture content of the white-pine fuel elements used in the testing is roughly 8%. The maximum amount of water which can be absorbed by the (commercial) white-pine toothpicks is roughly 30% of the dry toothpick

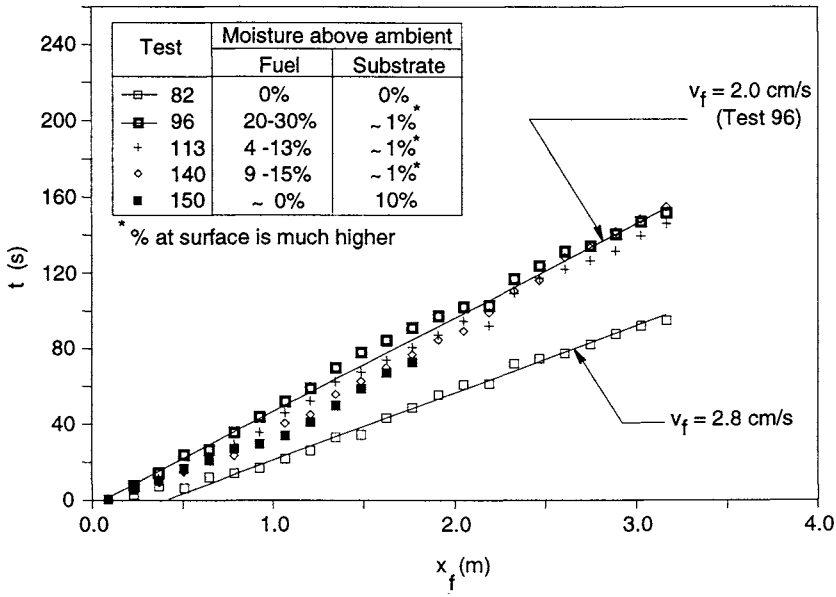

FIGURE 16 The streamwise centerline firefront position x_f as a function of the time t for tests with 0.55-m-wide beds of 4.6-cm-high white-pine toothpicks with pretest fuel loading m = 0.44 kg/m^2, at a wind speed U = 2.5 m/s. The moisture content is expressed as a mass percent above the initial mass (where the initial mass includes ambient moisture, typically 6 to 8% of the oven dry mass). The moisture enhancement is achieved by pretest confinement in a saturated environment.

mass, whereas chamise chaparral may have a ratio of water mass to dry mass of 40 to 50% in midsummer.

The rate of fire spread is substantially reduced when additional moisture (greater than ambient conditions) is added to the toothpicks or the substrate (Wolff *et al.*, 1991, Section 3.5; Figures 16 and 17). However, as noted earlier, our primary interest is the extreme fire spread conditions associated with Santa Ana wind episodes (after a long warm dry summer) during which the relative humidity may drop to ~10% or lower for days.

E. Substratum

The rate of fire spread observed in the laboratory testing appears to be independent of the substrate composition, at least for the clay and ceramic materials tested. The ceramic has density of 425 kg/m^3, heat capacity of 1130 J/(kg K), and thermal conductivity of 0.080 W/(m K) at 447 K and 0.223 W/(m K) at 1225 K. The respective properties of the clay are 1750 kg/m^3, 1000 J/(kg K),

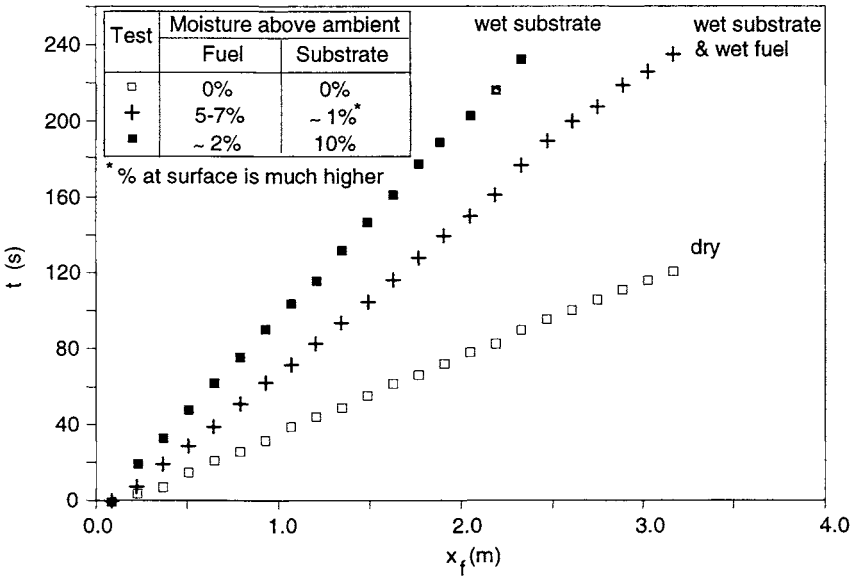

FIGURE 17 The same as Fig. 16, but for tests at a fuel loading $m = 0.22$ kg/m^2 and for a wind speed $U = 1.0$ m/s. The retardation of the rate of fire spread v_f owing to substrate moisture is distinguished roughly from the retardation owing to the fuel moisture content.

and 0.585 W/(m K) at room temperature. Although the square root of the conductance of the clay is about three times that of the ceramic at 1255 K, in fact the two inert materials yield about the same fire spread results. However, as just noted, retention of even residual liquid water by either material can lead to fire spread rate results distinctly altered from those obtained for the dry substrate.

V. TEST RESULTS FOR THE EFFECT OF WIND SPEED AND FUEL LOADING ON THE RATE OF FIRE SPREAD

As noted in Section III.D, and in accord with the results obtained from a diffusive-convective-preheating model in Section III.F, our laboratory testing with arrays of regularly arranged, upright, effectively identical white-pine toothpick-type discrete fuel elements gives good agreement with the formula (Figure 18)

$$v_f = C(U/m)^{1/2} \tag{29}$$

The premultiplier C is a function of H, d, inert content, water content, and bed width, but was not found to be a function of wood species within the limits of

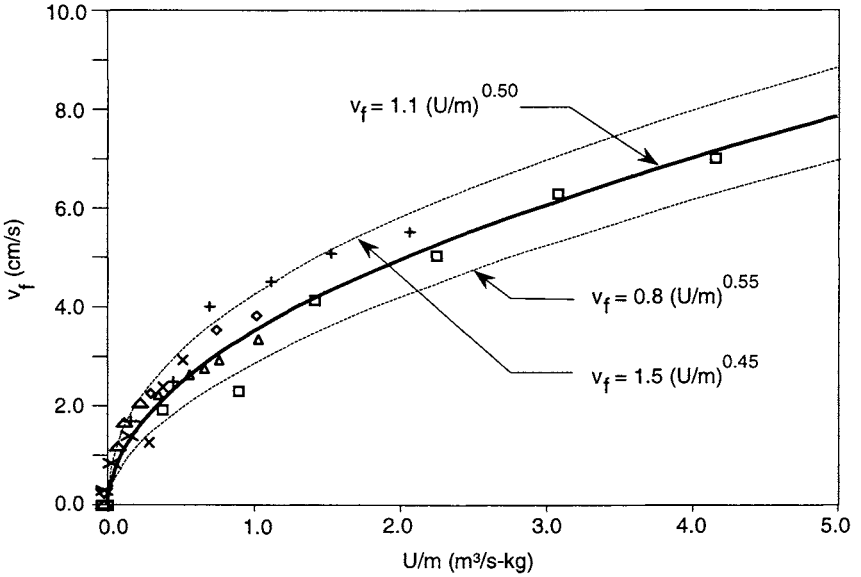

FIGURE 18 Quasi steady firefront propagation speed v_f through upright white-pine toothpicks as a function of the ratio of wind speed U to fuel loading m, from tests with $0 \leq U \leq 4.6$ m/s, 0.11 kg/m^2 $\leq m \leq$ 1.76 kg/m^2, and fuel-bed width $W = 0.55$ m.

our testing. The obviously finite range of the parameters U and m for which this formula has been shown to hold was stated in Section III.F.

In Section III.F, we showed that Eq. (29) is consistent with control of fire spread rate by convective-diffusive heat transfer from hot gas to unburned fuel elements. The dominance of the heat-transfer mechanism is anticipated to hold over some range $(U/m)_\ell < (U/m) < (U/m)_u$, where $(U/m)_\ell \to 0$, and $(U/m)_u$ was not encountered, for the range of parameters tested (Figure 18). At the upper limit, the forced-convective strain out of the burning of thin elements (Fendell, 1965), and/or the inefficiency of preheating downwind elements for too sparse loading probably intrudes. At the lower limit, the vigor of buoyant ascent, and/or the inaccessibility of sufficient oxygen for completion of fuel-vapor oxidation (Fendell and Kung, 1993), and/or the inefficiency of radiative preheating of downwind elements, may intrude, so the spread rate is small or nil.

A. Mixed Fuel Elements

If, for $U = 2.5$ m/s and $m \approx 0.42$ kg/m^2, one uses 4.4-mm-diameter elements to obtain the same fuel loading achieved with 1.3-mm elements, the spacing between elements is large for the thicker elements, and fire spread is not readily

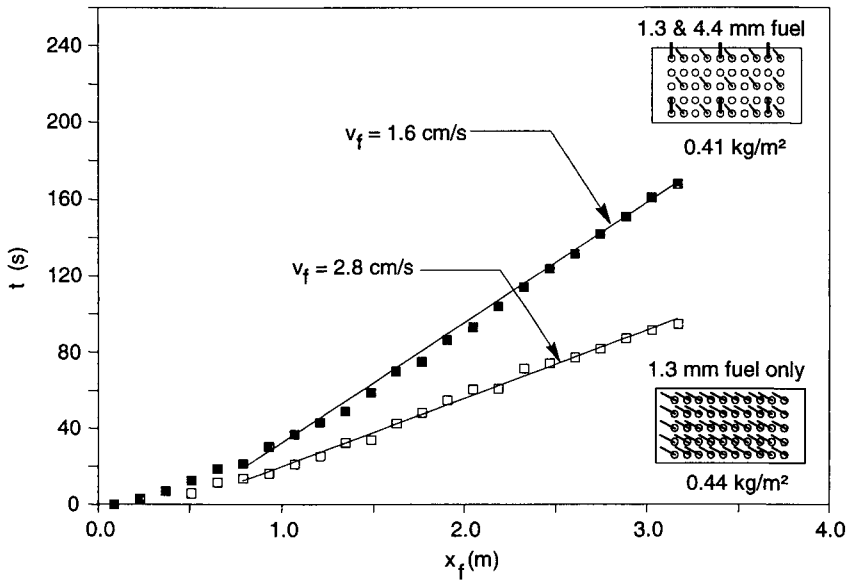

FIGURE 19 The streamwise centerline firefront position as a function of time for tests with a 0.55-m-wide bed, composed of 4.6-cm-high elements, at a wind speed $U = 2.5$ m/s. In the inset, empty circles designate an unfilled hole in the ceramic substrate, a vertical line denotes a hole occupied by a 4.4-mm-diameter birch dowel, and an inclined line denotes a hole occupied by a 1.3-mm-diameter white-pine toothpick.

sustained. This suggests that perhaps the thickness for elements to behave as thin fuel is below 4.4 mm. (The range between 3 and 6 mm is marginal.) Adding roughly 25% by mass of the thinner elements between the thicker elements facilitates sustained fire spread.

For example, Figure 19 juxtaposes a test involving 1.3-mm (27% by mass) and 4.4-mm (73% by mass) fuels, with a test involving entirely 1.3-mm-diameter fuel. The rate of fire spread in the mixed fuel bed is 1.6 cm/s, and in the thin-element-only bed, 2.8 cm/s. If we adopt the test with only thin fuel as a baseline and adopt a mass-weighted diameter of 3.6 mm for the mixed-fuel test, then (Wolff *et al.*, 1991) from the generalized relation (H is recalled to denote fuel-element height in the prefire bed)

$$v_f \sim \left(\frac{U}{m}\right)^{1/2}\left(\frac{H}{d}\right)^{p}, \qquad p \approx 2/3 \tag{30}$$

we obtain $v_f = 1.5$ cm/s—approximately what is observed. Since the multiplicative constant C is found to change significantly as specific fuel-element properties are altered (with m held constant), we must forsake some of the simplic-

ity of Eq. (29). If H and/or d vary from the nominal values used to assign C in Eq. (29), we must adopt Eq. (30).

Whereas both thick and thin fuel elements burned simultaneously in the just-discussed mixed-fuel test (Figure 19), in another test, only the thin fuel elements burned completely and a majority of the thicker fuel mass remained after firefront passage. The fuel loading was the same in both mixed-bed tests, but in the incomplete-burn test, all the thin toothpicks were moved to the columns between the columns with the thick elements. (By definition, a column consists of regularly spaced holes forming a straight line which is parallel to the oncoming-wind direction.) The wind speed was 2.5 m/s in the complete-burn test and 4.6 m/s in the incomplete-burn test. This example, in which a fire, in a bed with multidiameter fuel elements, consumed only the thinner elements and left the thicker elements virtually intact, mimics the burning of only those elements less than about 6 mm in thickness during firefront passage in wildland vegetation.

A bed of regularly arranged toothpicks is hardly a close surrogate for a chaparral stand, especially one that has experienced patch burning. Nevertheless, with respect to the pertinence of the just-described testing, in chaparral-type brush, we reiterate that most of the vegetation is consumed with firefront passage (Albini, 1992), especially for high-intensity fire (Pyne, 1984, p. 117). Furthermore, the range of height in southern California chaparral is limited to about 1.5–3 m, with 2 m being a typical characterization of mature chaparral. Also, because of the typical absence of much grazing, harvesting, "thinning," or patch burning in southern California, over large expanses the loading m increases with the passage of years, without high nonuniformity in the loading or size at a given time at a given site. Although the appellation (evergreen-shrub-type) chaparral admits the presence of multiple species, nevertheless large stands are often fairly uniform.

VI. CONCLUSIONS

On the chaparral-covered hillsides of southern California, autumnal episodes of persistent strong low-humidity warm winds, after the vegetation is desiccated during the long dry summer, can result in wind-aided fire spread over large areas. An annual critical fire season is encountered in other Mediterranean-climate locales on several continents.

To predict the evolution of the firefront that typically separates burned and unburned areas of vegetation, one could advance arc segments of the firefront perimeter. Each segment is to be advanced along its normal, according to the equilibrium rate of spread holding for the local, instantaneous conditions. This is to be carried out at the back and flanks of the perimeter, but it seems espe-

cially important to quantify accurately the advance of the head of the wind-aided fire.

In a plausible, semiempirical approach, the equilibrium rate of spread may be ascertained by reproducible, fast-turnaround laboratory testing of well-defined fuel beds in dedicated well-instrumented facilities, along with an integrated program of field burning. Simultaneously pursuing tractable, analytic, fundamentally sound models of the test phenomena may afford insight into the design of experiments and the interpretation of data.

Although the equilibrium rate of spread may not be fully achieved in the buildup phase of a firefront evolving from an ignition, for the high-spread-rate conditions of primary interest here, the fire in minutes typically achieves a size in which the equilibrium rate is an excellent approximation. Results from well-defined smaller scale experiments can be used to develop a capability to anticipate the evolution of the firefront configuration of a larger scale fire. It is this larger scale fire not suppressed in its early stage that challenges fire-management capacity at the urban-wildland interface.

However, by themselves, a limited number of minimally instrumented field events conducted in heterogeneous, possibly discontinuous, incompletely characterized fuel beds, which are burned under uncontrollable conditions, constitute isolated, perhaps unrepeatable anecdotes, not a data base to assist quantification.

NOTATION

Roman Symbols

c_b	specific heat capacity of a fuel bed	$\mathrm{J\ kg^{-1}\ K^{-1}}$
c_p	specific heat capacity at constant pressure of gas near the flame	$\mathrm{J\ kg^{-1}\ K^{-1}}$
D_1	(first) Damköhler number	
d	thickness of a combustible element in a fuel bed	m
F	firefront propagation speed	$\mathrm{m\ s^{-1}}$
g	gravity	$\mathrm{m\ s^{-2}}$
H	height of a fuel bed	m
h_i	ignition enthalpy	$\mathrm{J\ kg^{-1}}$
I	heat per area per time to preheat fuel (1-D model)	$\mathrm{J\ m^{-2}\ s^{-1}}$
k	thermal conductivity of gas	$\mathrm{J\ m^{-1}\ s^{-1}\ K^{-1}}$
k_b	thermal conductivity of a fuel bed	$\mathrm{J\ m^{-1}\ s^{-1}\ K^{-1}}$

L	flame length	m
m	thin-fuel loading burned during firefront passage	$kg\ m^{-2}$
n	number of fuel elements per unit area in a regular arrangement of upright fuel elements	m^{-2}
Q	effective exothermicity per mass of vegetative fuel burned	$J\ kg^{-1}$
$\dot{Q}$	line-fire intensity	$J\ m^{-1}\ s^{-1}$
$\dot{Q}_{crit}$	minimal line-fire intensity for fire spread	$J\ m^{-1}\ s^{-1}$
q	heat flux from gas phase downward to the preheating portion of a fuel bed	$J\ m^{-2}\ s^{-1}$
R	ratio characterizing presence of inert mass to combustible mass in a fuel bed	
s	distance between fuel elements in a regular arrangement	m
s	distance along a firefront perimeter	m
T_f	adiabatic flame temperature of pyrolyzate/air diffusion flame	K
T_i	ignition temperature	K
T_{pyr}	pyrolysis-onset temperature	K
T_∞	ambient temperature	K
t	time	s
U	ambient wind speed	$m\ s^{-1}$
U_{crit}	minimal ambient wind speed for fire spread	$m\ s^{-1}$
$(V_f)_i$	rate of change of x_i with time	$m\ s^{-1}$
v_f	rate of spread at the head of a wind-aided fire	$m\ s^{-1}$
W	updraft in a buoyant plume	$m\ s^{-1}$
x_i	coordinates of a point on the firefront perimeter ($i = 1, 2$)	m
x_1	x coordinate of a point on the firefront perimeter	m
x_2	y coordinate of a point on the firefront perimeter	m
x	Cartesian coordinate parallel to the ground	m
Y	stand-off distance (at the pyrolysis front), from the surface of the fuel bed, of the peak gas-phase temperature	m
y	Cartesian coordinate normal to the ground	m

GREEK SYMBOLS

α	Taylor entrainment constant	
β	rate of spread at the flank of a wind-aided fire	$m\ s^{-1}$
Γ	a reaction rate in Rothermel's theory	s^{-1}
$\Gamma(s, t)$	two-dimensional curve delineating firefront position	
ε	rate of spread at the back of a wind-aided fire	$m\ s^{-1}$
ε	small parameter describing diffusion	$m^2\ s^{-1}$
ε	radiative-absorption coefficient	m^{-1}
θ	angle subtended by the local outward normal to the firefront perimeter and the wind direction	
κ	local curvature of the firefront perimeter	m^{-1}
κ_b	effective thermal diffusivity of a fuel bed	$m^2\ s^{-1}$
ν_i	components of local outward normal vector to the firefront perimeter ($i = 1, 2$)	
ξ	fraction of exothermicity that serves to sustain propagation, in Rothermel's theory	
ρ_s	(true) density of vegetation	$kg\ m^{-3}$
ρ_b	bulk density of vegetation	$kg\ m^{-3}$
ρ_o	density of gas near the flame	$kg\ m^{-3}$
ρ_∞	ambient gas density	$kg\ m^{-3}$
σ	Stefan-Boltzmann constant	$J\ m^{-2} s^{-1}\ K^{-4}$
ϕ	porosity (voidage)	
ϕ_s	term to account for the effect of slope on the rate of head-fire spread, in Rothermel's model	
ϕ_w	term to account for the effect of wind on the rate of head-fire spread, in Rothermel's model	

ACKNOWLEDGMENTS

We are grateful to G. F. Carrier of Harvard University for his suggestions, guidance, and encouragement throughout our work on fire dynamics. We also thank F. A. Albini of Montana State University and S. J. Pyne of Arizona State University for many helpful comments on the manuscript.

RECOMMENDED READING

Albini, F. A. (1984). Wildland fires. *Amer. Scientist* **72**, 590–597.

Albini, F. A. (1992). Dynamics and modeling of vegetation fires: Observations. *In* "Fire in the Environment—The Ecological, Atmosphere, and Climatic Importance of Vegetation Fires" (P. J. Crutzen and J. G. Goldammer, Eds.), pp. 39–52. John Wiley, New York.

Carrier, G. F., Fendell, F. E., and Wolff, M. F. (1991). Wind-aided firespread across arrays of discrete fuel elements. I. Theory. *Combust. Sci. Tech.* **75**, 31–51.

Glassman, I. (1996). "Combustion," 3rd ed. Academic Press, New York.

Lyons, J. W. (1985). "Fire." Scientific American, New York.

Pyne, S. J. (1984). "Introduction to Wildland Fire—Fire Management in the United States." Wiley-Interscience, New York.

Wolff, M. F., Carrier, G. F., and Fendell, F. E. (1991). Wind-aided firespread across arrays of discrete fuel elements. II. Experiment. *Combust. Sci. Tech.* **77**, 261–289.

REFERENCES

Albini, F. A. (1984). Wildland fires. *Amer. Scientist* **72**, 590–597.

Albini, F. A. (1992). Dynamics and modeling of vegetation fires: observations. *In* "Fire in the Environment—The Ecological, Atmosphere, and Climatic Importance of Vegetation Fires" (P. J. Crutzen and J. G. Goldammer, Eds.), pp. 39–52. John Wiley, New York.

Anderson, D. H., Catchpole, E. A., de Mestre, N. J., and Parkes, T. (1982). Modeling the spread of grass fires. *J. Austral. Math. Soc. (Ser. B)* **23**, 451–466.

Anderson, H. E., and Rothermel, R. C. (1965). Influence of moisture and wind upon the characteristics of free-burning fires. *In* "Tenth Symposium (International) on Combustion," pp. 1009–1019. Combustion Institute, Pittsburgh.

Andrews, P. L. (1991). Use of the Rothermel fire spread model for fire danger rating and fire behavior prediction in the United States. *In* "Conference on Bushfire Modelling and Fire Danger Rating Systems—Proceedings" (N. P. Cheney and A. M. Gill, Eds.), pp. 1–8. CSIRO Division of Forestry, Yarralumla.

Burrows, N. D. (1999a). Fire behavior in jarrah forest fuels: 1. Laboratory experiments. *CALMScience* **3**(1), 31–56.

Burrows, N. D. (1999b). Fire behavior in jarrah forest fuels: 2. Field experiments. *CALMScience* **3**(1), 57–84.

Burrows, N., Ward, B., and Robinson, A. (1991). Fire behavior in spinifex fuels on the Gibson Desert Nature Reserve, Western Australia. *J. Arid Environments* **20**, 189–204.

Beer, T. (1990). The Australian national bushfire model project. *Mathematical and Computer Modeling* **13**(12), 49–56.

Beer, T. (1991). Bushfire-control decision support systems. *Environment International* **17**, 101–110.

Carrier, G., Fendell, F., Chen, K., and Cook, S. (1991). Evaluating a simple model for laminar-flame-propagation rates. II. Spherical geometry. *Combust. Sci. Tech.* **79**, 229–245.

Carrier, G. F., Fendell, F. E., and Wolff, M. F. (1991). Wind-aided firespread across arrays of discrete fuel elements. I. Theory. *Combust. Sci. Tech.* **75**, 31–51.

Catchpole, W. R., Catchpole, E. A., Butler, B. W., Rothermel, R. C., Morris, G. A., and Latham, D. J. (1998). Rate of spread of free-burning fires in woody fuels in a wind tunnel. *Combust. Sci. Tech.* **131**, 1–37.

Cheney, N. P. (1981). Fire behavior. *In* "Fire and the Australian Biota" (A. M. Gill, R. H. Groves, and I. R. Noble, Eds.), pp. 151–175. Australian Academy of Science, Canberra.

Cheney, P., and Sullivan, A. (1997). "Grassfires—Fuel, weather and fire behavior." CSIRO, Collingwood.

Christensen, K., Flyvbjerg, H., and Olami, Z. (1993). Self-organized critical forest-fire model: Mean-field theory and simulation in 1 to 6 dimensions. *Phys. Rev. Let.* **71**, 2737–2740.

Chorin, A. J. (1980). Flame advection and propagation algorithms. *J. Comp. Phys.* **35**, 1–11.

Coleman, J. R., and Sullivan, A. L. (1996). A real-time computer application for the prediction of fire spread across the Australian landscape. *Simulation* **67**, 230–240.

de Ris, J. (1979). Fire radiation—a review. *In* "Seventeenth Symposium (International) on Combustion," pp. 1003–1016. Combustion Institute, Pittsburgh.

Emmons, H. W. (1963). Fire in the forest. *Fire Abstr. Revs.* **5**, 163–178.

Emmons, H. W. (1965). Fundamental problems of the free burning fire. *In* "Tenth Symposium (International) on Combustion," pp. 951–964. Combustion Institute, Pittsburgh.

Emmons, H. W. (1971). Fluid mechanics and combustion. *In* "Thirteenth Symposium (International) on Combustion," pp. 1–18. Combustion Institute, Pittsburgh.

Fendell, F. E. (1965). Ignition and extinction in combustion of initially unmixed reactants. *J. Fluid Mech.* **21**, 281–303.

Fendell, F. E., and Kung, E. Y. (1993). The pyrolyzation of vegetation by brief intense radiation. *J. Thermophys. Heat Transf.* **7**, 510–516.

Finney, M. A. (1998). FARSITE: fire area simulator—model development and evaluation. Research Paper RMRS-RP-4. USDA Forest Service, Rocky Mountain Research Station, Fort Collins.

Fleeter, R. D., Fendell, F. E., Cohen, L. M., Gat, N., and Witte, A. B. (1984). Laboratory facility for wind-aided firespread along a fuel matrix. *Combust. Flame* **57**, 289–311.

Fons, W. L. (1946). Analysis of fire spread in light forest fuels. *J. Agric. Res.* **72**, 93–121.

Frandsen, W. H. (1971). Firespread through porous fuels from the conservation of energy. *Combust. Flame* **16**, 99–16.

Gill, A. M., Burrows, N. D., and Bradstock, R. A. (1995). Fire modeling and fire weather in an Australian desert. *CALMScience (W. Australian J. Conservation Land Management)* **24** (Supplement 4), 29–34.

Goldstein, P. (1995). The wise man of the mountains. *Los Angeles Times Mag.* (Feb. 12), 20–23, 33–34, 36.

Gould, J. S. (1991). Validation of the Rothermel firespread model and related fuel parameters in grassland fires. *In* "Conference on Bushfire Modelling and Fire Danger Rating Systems—Proceedings" (N. P. Cheney and A. M. Gill, Eds.), pp. 51–64. CSIRO Division of Forestry, Yarralumla.

Knight, I., and Coleman, J. (1993). A fire perimeter expansion algorithm based on Huygens' wavelet propagation. *Int. J. Wildland Fire* **3**, 73–84.

Luke, R. H., and McArthur, A. G. (1978). "Bushfires in Australia." Australian Government Publishing Service, Canberra.

Markstein, G. H. (1964). Perturbation analysis of stability and response of plane flame fronts. *In* "Nonsteady Flame Propagation" (G. H. Markstein, Ed.), pp. 15–74. Pergamon, New York.

Marsden-Smedley, J. B., and Catchpole, W. R. (1995). Fire behavior modelling in Tasmanian buttongrass moorlands. II. Fire behavior. *Int. J. Wildland Fire* **5**, 215–228.

Minnich, R. A. (1998). Landscapes, land-use and fire policy: Where do large fires come from. *In* "Large Forest Fires" (J. M. Moreno, Ed.), pp. 133–158. Bookhuys, Leiden.

Mongia, L. M., Pagni, P. J., and Weise, D. R. (1998). "Model Comparisons with Simulated Wildfire Flame Spread Data." Western States Section Spring Meeting, Paper WSS/CI 985–68. Combustion Institute, Pittsburgh.

Nelson, R. M., and Adkins, C. W. (1988). A dimensionless correlation for the spread of wind-driven forest fires. *Can. J. For. Res.* **18**, 391–397.

Osher, S., and Sethian, J. A. (1988). Fronts propagating with curvature-dependent speeds: Algorithms based on Hamilton-Jacobi formulations. *J. Comput. Phys.* **79**, 12–49.

Pitts, W. M. (1991). Wind effects on fire. *Prog. Energy Combust. Sci.* **17**, 83–134.
Pyne, S. J. (1982). "Fire in America—A Cultural History of Wildland and Rural Fire." Princeton University Press, Princeton.
Pyne, S. J. (1984). "Introduction to Wildland Fire—Fire Management in the United States." Wiley-Interscience, New York.
Pyne, S. J. (1991). "Burning Bush—A Fire History of Australia." Henry Holt, New York.
Pyne, S. J. (1995). "World Fire—The Culture of Fire on Earth." Henry Holt, New York.
Pyne, S. J., Andrews, P. L., and Laven, R. D. (1996). "Introduction to Wildland Fire," 2nd ed. John Wiley, New York.
Reid, R. (1994). After the fire. *Amer. Scientist* **82** (1; Jan.–Feb.), 20–21.
Richards, G. D. (1993). The properties of elliptical wildfire growth for time-dependent fuel and meteorological conditions. *Combust. Sci. Tech.* **92**, 145–171.
Roberts, S. (1989). "A Line Element Algorithm for Curve Flow Problems in the Plane." Center for Mathematical Analyses Report CMA-R58-89. Australian National University, Canberra.
Rothermel, R. C. (1972). "A Mathematical Model for Predicting Firespread in Wildland Fuels." Research Paper INT-115. USDA Forest Service, Intermountain Forest and Range Experiment Station, Ogden.
Sethian, J. A. (1996). "Level Set Methods—Evolving Interfaces in Geometry, Fluid Mechanics, Computer Vision, and Materials Science." Cambridge University, Cambridge.
Steward, F. R. (1974). Firespread through a fuel bed. *In* "Heat Transfer in Fires: Thermophysics/Social Aspects/Economic Impact" (P. L. Blackshear, Ed.), pp. 315–378. Scripta, Washington.
Steward, F. R., and Tennankore, K. N. (1979). "Fire Spread and Individual Particle Burning Rates For Uniform Fuel Matrices." Report, Fire Science Center. University of New Brunswick, Fredericton.
Taylor, G. I. (1961). Fire under influence of natural convection. *In* "International Symposium on the Use of Models in Fire Research" (W. G. Berl, Ed.), Publication 786, pp. 10–28. National Academy of Sciences—National Research Council, Washington, DC.
Thomas, P. H. (1971). Rates of spread of some wind-driven fires. *Forestry* **44**, 155–175.
Weber, R. O. (1991). Modeling firespread through fuel beds. *Prog. Energy Combust. Sci.* **17**, 67–82.
Weber, R. O., and de Mestre, N. J. (1991). Buoyant convection: a physical process as the basis for fire modeling. *In* "Conference on Bushfire Modelling and Fire Danger Rating Systems—Proceedings" (N. P. Cheney and A. M. Gill, Eds.), pp. 43–50. CSIRO Division of Forestry, Yarralumla.
Weise, D. R. (1993). "Modeling Wind and Slope-Induced Wildland Fire Behavior." PhD dissertation. University of California, Berkeley.
Williams, F. A. (1977). Mechanisms of firespread. *In* "Sixteenth Symposium (International) on Combustion," pp. 1281–1294. Combustion Institute, Pittsburgh.
Wolff, M. F., Carrier, G. F., and Fendell, F. E. (1991). Wind-aided firespread across arrays of discrete fuel elements. II. Experiment. *Combust. Sci. Tech.* **77**, 261–289.